

PROPAGATION OF THE WAVE FRONT ON  
UNTRANSPOSED OVERHEAD AND UNDERGROUND TRANSMISSION LINES

by

LEE KAI-CHUNG

B.Sc., University of Wisconsin, 1973  
M.Sc., University of British Columbia, 1975

A THESIS SUBMITTED IN PARTIAL FULFILMENT OF  
THE REQUIREMENT FOR THE DEGREE OF  
MASTER OF APPLIED SCIENCE

in the Department

of

Electrical Engineering

We accept this thesis as conforming  
to the required standard

THE UNIVERSITY OF BRITISH COLUMBIA

April, 1977

(c)

Lee Kai-Chung, 1977.

In presenting this thesis in partial fulfilment of the requirements for an advanced degree at the University of British Columbia, I agree that the Library shall make it freely available for reference and study.

I further agree that permission for extensive copying of this thesis for scholarly purposes may be granted by the Head of my Department or by his representatives. It is understood that copying or publication of this thesis for financial gain shall not be allowed without my written permission.

Department of Electrical Engg

The University of British Columbia  
2075 Wesbrook Place  
Vancouver, Canada  
V6T 1W5

Date May 2, 77,

## ABSTRACT

The propagation of the switching surge wave front on multiphase power lines was investigated by modal analysis and conventional Fourier Transformation. A 500 kV untransposed, three-phase transmission line, for which field test results were available, was chosen as a test case.

Phase A of this test line was excited from a double exponential voltage source and the voltage response at the receiving end was calculated and measured in all three phases. The calculated voltage arrival time matched closely the measured value, and was very close to the time taken by electromagnetic waves in air at a speed of  $0.3 \text{ km}/\mu\text{s}$ . The calculated voltage response curves also came close to the measured results (errors within 8%).

## TABLE OF CONTENTS

ABSTRACT . . . . .	ii
TABLE OF CONTENTS . . . . .	iii
LIST OF ILLUSTRATIONS . . . . .	v
ACKNOWLEDGEMENTS . . . . .	vi
INTRODUCTION . . . . .	1
CHAPTER I COMPUTATION OF LINE CONSTANTS . . . . .	
1. Introduction . . . . .	3
2. Transmission Line Data . . . . .	3
3. Line Parameter Calculation . . . . .	6
4. Calculations of Skin Effect in Conductors . . . . .	10
5. Output from Line Constants Program . . . . .	13
6. Positive and Zero Sequence Parameters . . . . .	19
CHAPTER II COMPUTATION OF TRANSFERFUNCTION FOR FREQUENCY	
RESPONSE OF TEST LINE . . . . .	
1. Introduction . . . . .	22
2. Outline of the Theory Used in the Transfer Function Program . . . . .	22
3. Inclusion of Boundary Conditions at Sending End . . . . .	28
4. Transfer Function for Test Line . . . . .	32
CHAPTER III TIME RESPONSE OF TEST LINE THROUGH FOURIER	
TRANSFORMATION . . . . .	
1. Introduction . . . . .	36
2. Numerical Fourier Transformation of Input Voltage from Time to Frequency Domain . . . . .	36

3. Output Voltage in Frequency Domain . . . . .	40
4. Output Voltage in Time Domain by Numerical Inverse Fourier Transformation . . . . .	41
5. Numerical Aspects of Fourier Transformation Program . . . . .	43
CHAPTER IV DUPLICATION OF FIELD TESTS . . . . .	
1. Doubling Effect on Open-Ended Line . . . . .	49
2. Comparison With Field Measurements and Other Simulation Results . . . . .	50
CHAPTER V CONCLUSIONS . . . . .	54
APPENDIX 1 Transfer Function Program Listings . . . . .	55
APPENDIX 2 Phase Smoothing Program Listings . . . . .	61
APPENDIX 3 Fourier Transformation Program Listings . . . . .	62
BIBLIOGRAPHY . . . . .	68

## LIST OF ILLUSTRATIONS

Figure	Page
1. Overall scheme of programmes used . . . . .	2
2. Transmission line geometry . . . . .	4
3. Line parameter calculation . . . . .	7
4. Skin effect on resistance and internal inductance of each bundled conductor by Galloway's formula and tubular conductor formula . . . . .	11
5. Elements of the resistance matrix of the test line, with Galloway's formula and the formula for the tubular conductor, for skin effect . . . . .	17
6. Elements of the reactance matrix of the test line, with Galloway's formula and the formula for the tubular conductor, for skin effect . . . . .	18
7. Change in sequence resistance due to change in conductor bundle resistance . . . . .	20
8. Transmission line configuration with boundary conditions . . . . .	23
9. Magnitude of transfer functions with skin effect calculation by Galloway's formula and by tubular conductor formula . . . . .	33
10. Phase of transfer functions (Identical results with skin effect calculation by Galloway's formula and by tubular conductor formula) . . . . .	34
11. Linear interpolation of input voltage in time domain . .	38
12. Linear interpolation of output voltage in time domain . .	38
13. Input voltage and calculated output voltage with $H(\omega) = 1.0 \angle 0^\circ$ . . . . .	45
14. Same test as in Fig. 13 from 0.1 to 15 ms. . . . .	46
15. Output voltage at receiving end of transmission line . .	52
16. Output voltage at receiving end of transmission line with field measurement and other simulation results . . .	55

## ACKNOWLEDGEMENT

I would like to thank my thesis supervisor, Professor Hermann W. Dommel for supplying the topic, for valuable criticism and advise, and for countless hours of discussions during the research work and writing up of this thesis. Also, I would like to show appreciation to Dr. Dommel for providing the Line Constants Program and an initial version of the Fourier Transform program.

I would also like to thank the thesis co-reader, Professor Malcome D. Wong for proof-reading this thesis and offering further suggestions.

I am also grateful to Mr. King K. Tse for providing the initial version of the Transfer Function Program and helpful discussions about the programme during the early part of the research.

The financial support of The University of British Columbia is also gratefully acknowledged.

Special thanks are expressed to Mrs. Semmens in the Electrical Engineering main office for producing this excellently typed thesis from my semi-legible handwriting.

Finally, I am indebted to my parents and my wife for their tireless encouragement and patience.

## INTRODUCTION

The attenuation and distortion of wave fronts on single circuit multiphase transmission lines or underground cables was investigated. The purpose of this work was useful for surge insulation coordination study. The solution methods were applied to the specific case of a 500 kV untransposed overhead line, for which test results were available.<sup>1,2\*</sup> This line is part of the 500 kV Azumi Trunk transmission link of the Tokyo Electric Power System in Japan. In the field tests, the sending end of the line was energized with a double exponential surge wave of the form  $v(t)=k(e^{-\alpha_1 t} - e^{-\alpha_2 t})$ , as a representation of surge phenomenon on a line eg. lightning surge, from an impulse generator<sup>3</sup> through a series resistance of  $415\Omega$ . In the computer simulation, this double exponential input wave as well as other forms of input voltages, such as single exponential decay wave, triangular waves, step wave and delta wave were also studied.

The way in which computer programmes were used for the analysis in this thesis is illustrated in Fig. 1. The Line Constants Program (LCP) was first used to give the distributed line parameters from the tower geometry and conductor characteristics as a function of frequency. Then, the Transfer Function Program (TFP) was used to obtain the output voltage at the receiving end (83.212 km from sending end) for all frequency points. After the transfer functions at discrete frequency points were obtained, the Fourier Transform Program (FTP) was used to find the voltage at the receiving end as a function of time for any form of input voltage.

In the Fourier Transform Program, linear interpolation between

\* The superscripts denote reference numbers in the bibliography.

successive data points were used in the time domain as well as in the frequency domain. For the 500 kV line used as an example, a density of 20 points per decade on the frequency scale gave sufficiently accurate results.

The computation of the voltage response in three phases at the receiving end with any one of the phases energized at the sending end would take about 80 s. CPU time on the UBC IBM 370/168 computer system at a cost of approximately CC\$30. For a more general case of three input voltages on all three phases, only a slight modification in the Transfer Function Program would be required to obtain the results.

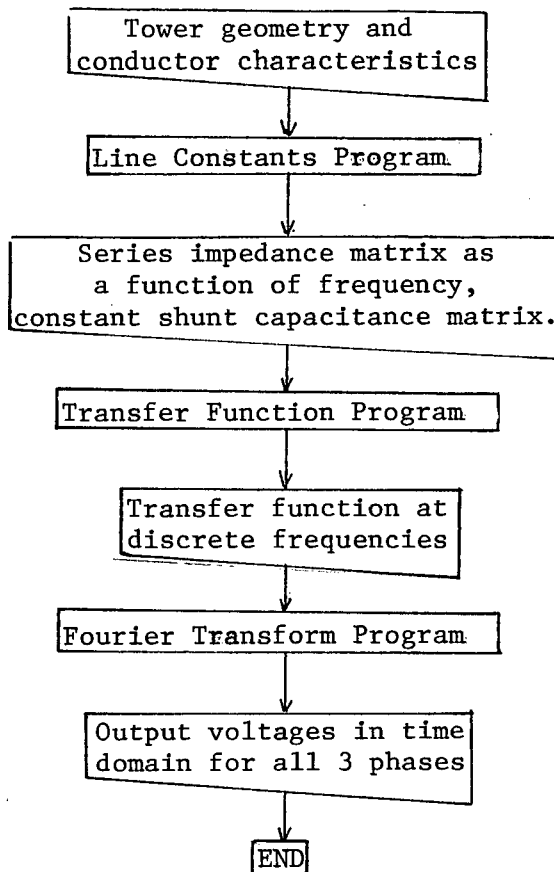


Fig. 1. Overall scheme of program used.

## CHAPTER I

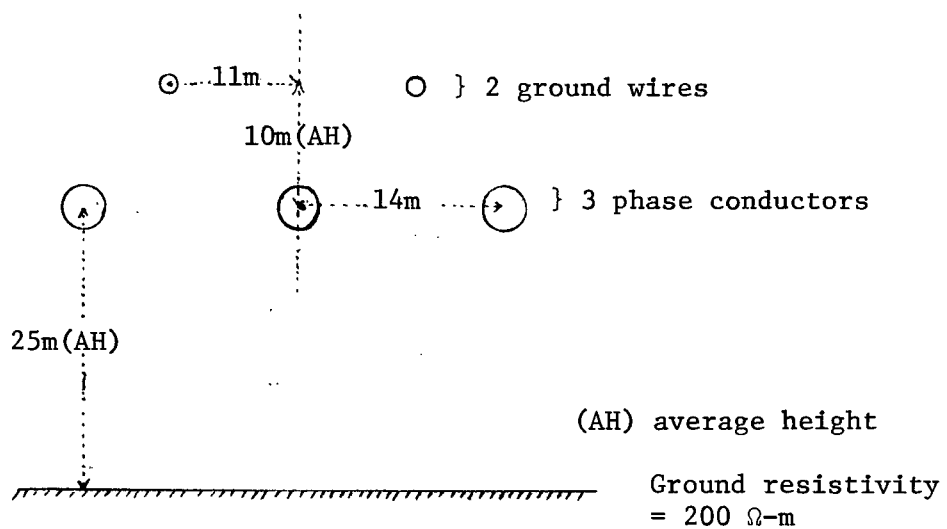
## COMPUTATION OF LINE CONSTANTS

## 1. Introduction

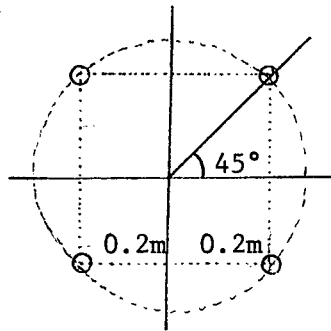
The program which was used for the calculation of line parameters is a modified version of the Line Constants Program written by H. W. Dommel<sup>4,5</sup>. It calculates the frequency-dependent series impedance matrix and the constant shunt capacitance matrix for overhead lines from the given tower geometry and conductor characteristics at specified frequency points. For the analysis of underground cables, this program would have to be replaced by a cable constants program. The value of the impedance and capacitance matrices is needed for the Transfer Function Program to obtain the transfer functions at the specified frequency points.

## 2. Transmission Line Data

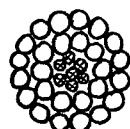
The transmission line used as an example for this simulation study is part of the 500 kV Azumi-Trank transmission link of the Tokyo Electric Power System in Japan<sup>1,2</sup>. This is a three-phase untransposed line with two ground wires. Each phase is a bundle conductor with four steel-reinforced aluminum cables (see Fig. 2). The tower geometry and conductor characteristics are listed in Table 1. The conductor characteristics were taken from the German standard DIN 48204 because they were not defined in enough detail in the description of the field tests<sup>4,5</sup>.



- a) Tower geometry (height is average height above ground, not height at tower location).



- b) Bundle conductors of each phase



○ Aluminum strands  
⊗ Steel strands

- c) 26 Al./7st. Steel-reinforced aluminum cable used for ground wires and phase conductors

Fig. 2 Transmission line geometry

TABLE I  
TRANSMISSION LINE DATA

General data

Length of transmission line	= 83.212 km
Average height above ground of three phase conductors (flat configuration)	= 25 m
Average height above ground of ground wires	= 35 m
Earth resistivity (presumably farmland)	= 200 $\Omega \cdot m$
Resistivity of aluminum	= $3.21 \times 10^{-8} \Omega \cdot m$
Relative permeability of aluminum ( $\mu_r$ )	= 1.0
Permeability of aluminum ( $\mu_0 \mu_r$ )	= $4\pi \times 10^{-8} H/m$

Details for ground wire

Type:	Steel-reinforced aluminum cable, as shown in Fig. 2c.
Total no. of aluminum strands	= 26
No. of aluminum strands in outer layer of conductor	= 16
Steel core diameter	= 5.85 mm
Outside diameter of conductor	= 15.7 mm
D.C. resistance at 20°C	= 0.262 $\Omega/km$

Details of phase conductor

Type:	Steel-reinforced aluminum cable as shown in Fig. 2c, with conductors in each phase as shown in Fig. 2b
Total no. of aluminum strands	= 26
No. of aluminum strands in outer layer of conductor	= 16
Steel core diameter	= 8.1 mm
Outside diameter of conductor	= 21.7 mm
D.C. resistance at 20°C	= 0.136 $\Omega/km$

### 3. Line Parameter Calculation

(i) Series impedance matrix - Carson's formula<sup>6,2</sup> is used for calculating the impedances of the conductor earth return loops. Earth conductivity is assumed to be uniform and the earth plane is assumed to be flat and parallel to the conductors. Also, spacings between conductors are assumed to be large compared with conductor radii, that is, proximity effects are ignored. The elements of the impedance matrix  $[Z_{ij}]$  are given as

$$Z_{ii} = (R_{ii} + \Delta R_{ii}) + j(2\omega 10^{-4} \ln \frac{2h_i}{GMR_i} + \Delta X_{ii}) \Omega/km$$

$i = 1, \dots, N$  (1-1)

and  $Z_{ij} = Z_{ji}$

$$= \Delta R_{ij} + j(2\omega 10^{-4} \ln \frac{s_{ij}}{s_{ij}} + \Delta X_{ij}) \Omega/km$$

$j = 1, \dots, N; i = 1, \dots, N; i \neq j,$  (1-2)

where  $R_{ii}$  = resistance of  $i^{\text{th}}$  conductor in  $\Omega/km$  (see section 4.  
on skin effect)

$h_i$  = average height above ground of  $i^{\text{th}}$  conductor in m,

$s_{ij}$  = distance between  $i^{\text{th}}$  conductor and ground image of  
 $j^{\text{th}}$  conductor in m (see Fig. 3),

$s_{ij}$  = distance between  $i^{\text{th}}$  and  $j^{\text{th}}$  conductors in m  
(see Fig. 3),

$GMR_i$  = geometric mean radius of  $i^{\text{th}}$  conductor in m,

$\omega$  = angular frequency,

$\Delta R$  = correction terms in resistance for earth return effect,

$\Delta X$  = correction terms in resistance for earth return effect.

Carson's correction terms  $\Delta R$  and  $\Delta X$  are functions of the angle

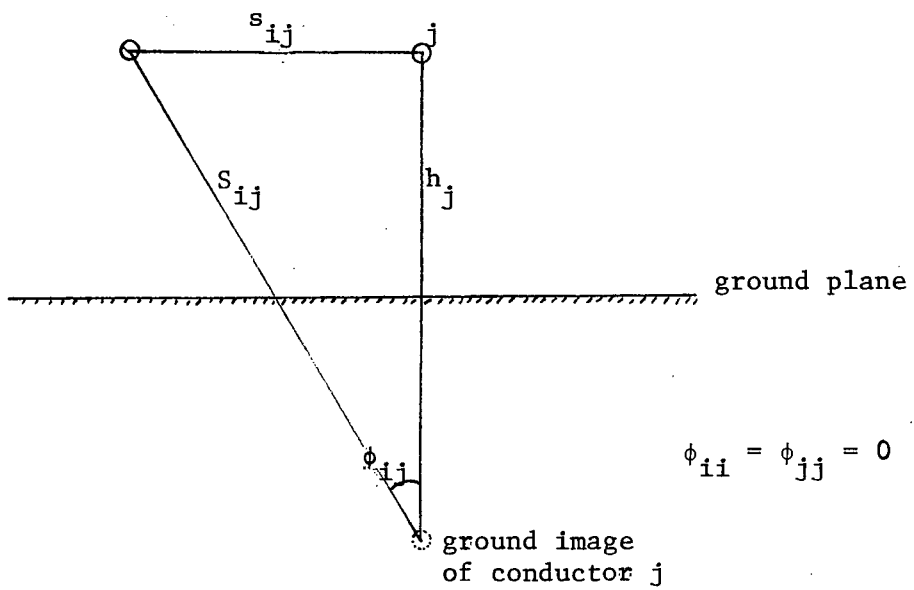


Fig. 3 Line parameter calculation

$\phi_{ij}$  (see Fig. 3) and of the parameter

$$a = ks \int_0^f$$

where  $k = 4\pi\sqrt{5} \times 10^{-4}$

$$s = \begin{cases} 2h_i & \text{for self impedance} \\ S_{ij} & \text{for mutual impedance} \end{cases}$$

$\rho$  = earth resistivity in  $\Omega \cdot m$

$f$  = frequency in Hz

For numerical calculations, Carson's integral for  $\Delta R$  and  $\Delta X$  has been developed into an infinite series<sup>4</sup>, which is used for  $a \ll 5$ ,

$$\begin{aligned} \Delta R' = 4\omega 10^{-4} & \left\{ \frac{\pi}{8} - b_1 a \cos \phi + b_2 [(c_2 - 1na)a^2 \cos 2\phi + \phi a^2 \sin 2\phi] \right. \\ & + b_3 a^3 \cos 3\phi - d_4 a^4 \cos 4\phi \\ & - b_5 a^5 \cos 5\phi + b_6 [(c_6 - 1na)a^6 \cos 6\phi + \phi a^6 \sin 6\phi] \\ & + b_7 a^7 \cos 7\phi - d_8 a^8 \cos 8\phi \\ & \left. - \dots \right\} \end{aligned} \quad (1-3a)$$

$$\begin{aligned} \Delta X' = 4\omega 10^{-4} & \left\{ \frac{1}{2} (0.6159315 - 1na) + b_1 a \cos \phi - d_2 a^2 \cos 2\phi \right. \\ & + b_3 a^3 \cos 3\phi - b_4 [(c_4 - 1na)a^4 \cos 4\phi + \phi a^4 \sin 4\phi] \\ & + b_5 a^5 \cos 5\phi - d_6 a^6 \cos 6\phi + b_7 a^7 \cos 7\phi \\ & - b_8 [(c_8 - 1na)a^8 \cos 8\phi + \phi a^8 \sin 8\phi] \\ & \left. + \dots \right\} \end{aligned} \quad (1-3b)$$

where  $b_i$ ,  $c_i$  and  $d_i$  are constants given by

$$b_1 = \frac{\sqrt{2}}{6} \text{ for odd subscripts } i$$

$$b_2 = \frac{1}{16} \text{ for even subscripts } i$$

$$b_i = b_{i-2} \frac{\text{sign}}{i(i+2)}, \quad i > 2$$

with sign = {  
+1,  $i = 1, 2, 3, 4, 9, 10, 11, 12, \dots$   
-1,  $i = 5, 6, 7, 8, 13, 14, 15, 16, \dots$

and  $c_2 = 1.3659315$

$$c_i = c_{i-2} + \frac{1}{i} + \frac{1}{i+2}, i > 2$$

and  $d_i = \frac{\pi}{4} b_i$

Note that from eqtns (1-3a) and (1-3b), each 4 terms in  $i = 1, 4$  form a repetitive group in the infinite series.

For  $a > 5$ , the approximation formulae given by Butterworth<sup>7,2</sup> is used, instead of the infinite series

$$\Delta X = \left( \frac{\cos \phi}{a} - \frac{\cos 3\phi}{a^3} + \frac{3 \cos 5\phi}{a^3} + \frac{45 \cos 7\phi}{a^7} \right) \frac{4\omega 10^{-4}}{\sqrt{2}} \quad (1-4a)$$

$$\Delta R = \left( \frac{\cos \phi}{a} - \frac{\sqrt{2} \cos 2\phi}{a^2} + \frac{\cos 3\phi}{a^3} + \frac{3 \cos 5\phi}{a^5} - \frac{45 \cos 7\phi}{a^7} \right) \frac{4\omega 10^{-4}}{\sqrt{2}} \quad (1-4b)$$

Note that the infinite series for  $R$  and  $X$  derived from Carson's integrals will only converge after about 10 or more terms if  $a > 3$ . The first few terms are highly oscillating in that case.

(ii) Shunt capacitance matrix  $[C]$  - The capacitance matrix  $[C]$  is the inverse of the potential coefficient matrix  $[P]$ .

$$[C] = [P]^{-1}$$

The matrix element of  $[P]$  can easily be obtained from the tower geometry,

$$P_{ii} = 2c^2 \times 10^{-4} \ln \frac{2h_i}{r_i} \text{ km/F} \quad (1-5)$$

and  $P_{ij} = 2c^2 \times 10^{-4} \ln \frac{s_{ij}}{s_{ij}} \text{ km/F}$  (1-6)

where  $r_i$  = radius of conductor in m

$c$  = velocity of light in km/s

Eqtions (1-5) and (1-6) are valid as long as  $r_i$  (0.02 m in the example) is much smaller than spacings between conductors (14 m in the

example). Note that the elements of the shunt capacitance matrix are only dependent on the tower geometry and are not dependent on frequency. This is an approximation which is valid for frequencies up to approximately 1 MHz, where earth correction terms for capacitances are not yet important<sup>8</sup>.

#### 4. Calculations of Skin Effect in Conductors

The skin effect in the earth return is accounted for by Carson's formula. While the earth return skin effect has a major influence on line parameters, skin effect in the conductors must also be considered at higher frequencies. As frequency increases, the current flows more and more on the surface of the conductor. This can be described by the nominal depth of penetration of current ( $\delta$ ) as given by<sup>9</sup>

$$\delta = \sqrt{\frac{\rho_c}{\pi f \mu}}$$

where

$\rho_c$  = resistivity of conductor material in  $\Omega \cdot \text{m}$

$\mu$  = absolute magnetic permeability in  $\text{H/m}$

f = frequency in Hz

Since the current is confined to the surface of the conductor at high frequencies, the conductor resistance increases and the internal inductance decreases with frequency (see Fig. 4). In eqtn (1-1), the self inductance matrix element

$$L_{ii} = 2 \times 10^{-4} \ln \frac{2h_i}{GMR_i} \quad \text{H/km} \quad (1-8)$$

is the resultant of the internal and external inductance, i.e.

$$L_{ii} = 2 \times 10^{-4} \ln \frac{r_i}{GMR_i} + 2 \times 10^{-4} \ln \frac{2h_i}{r_i} \quad \text{H/km} \quad (1-9)$$

The first and second term in eqtn (1-9) is due to the flux inside and outside the conductor, respectively. Note that the first term (internal inductance) is small compared to the second term for high voltage overhead lines at low frequencies and vanishes completely at high frequencies.

Skin effect on resistance and internal inductance of each bundled conductor by Galloway's formula and tubular conductor formula

Resistance  $R$  ( $\Omega/\text{km}$ )

Internal reactance  $X_1$  ( $\Omega/\text{km}$ )

Inductance  $L$  ( $\text{H}$ )

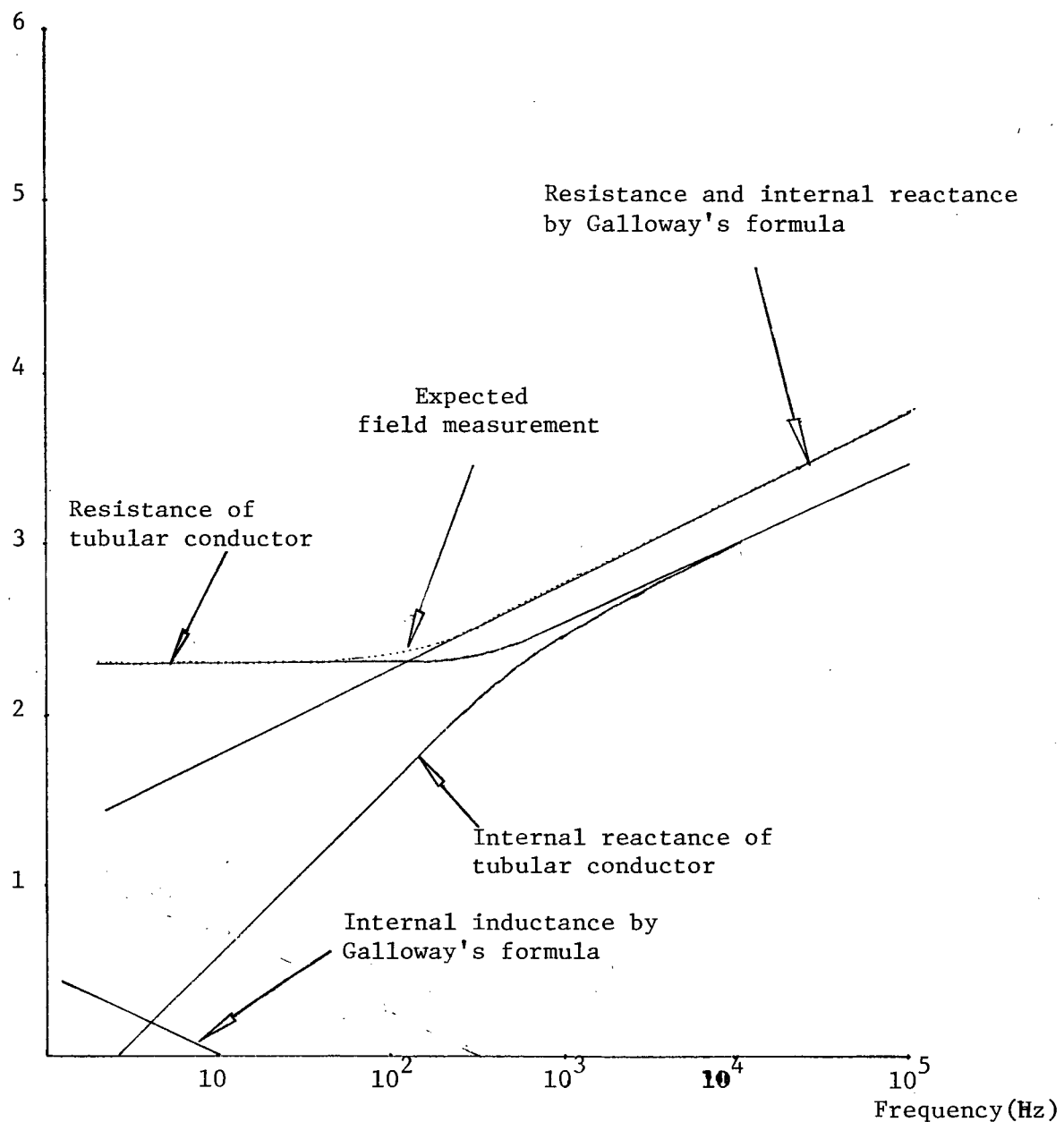


Fig. 4

Thus, the skin effect on the total inductance is normally negligible over the entire frequency range. However, the skin effect on resistance is quite pronounced.

The skin effect on the conductor resistance and internal reactance was calculated in two ways. With the first method, the conductor was treated as a solid tubular aluminum conductor of the same cross-sectional area as the actual conductor. The steel core was completely ignored. This was recommended as a reasonable approximation. The formula for the internal impedance of a tubular conductor of nonmagnetic material is<sup>10,4</sup>

$$\begin{aligned} Z_{\text{internal}} &= \frac{R_{\text{conductor}} + j\omega L_{\text{internal}}}{R_{dc}} \\ &= \frac{j\frac{1}{2}mr(1-s^2)(ber(mr)+jbei(mr))+\phi(ker(mr)+jkei(mr))}{(ber'(mr)+jbei'(mr))+\phi(ker'(mr)+jkei'(mr))} \end{aligned} \quad (1-10)$$

where

$$\phi = -\frac{ber'(mq)+jbei'(mq)}{ker'(mq)+jkei'(mq)}$$

$R_{dc}$  = d.c. resistance of conductor in  $\Omega/\text{km}$

$r$  = outside radius of conductor in m

$q$  = outside radius of steel core in m

$$s = \frac{q}{r}$$

$$(mr) = \left(\frac{k}{1-s^2}\right)^{1/2}$$

$$(mq) = \left(\frac{ks}{1-s^2}\right)^{1/2}$$

and

$$k = \frac{8\pi 10^{-4}f}{R_{dc}}$$

The expressions  $ber(...)+jbei(...)$ ,  $ber'(...)+jbei'(...)$ ,  $ker(...)+jkei(...)$  and  $ker'(...)+jkei'(...)$  are modified Bessel functions, which can be evaluated by polynomial approximation<sup>11,4</sup>. An empirical formula

for conductor resistance and conductor internal reactance was developed by Galloway<sup>12</sup>, which is based on measurements in the electrolytic tank. In this approach, current is assumed to be confined to the outer layer strands (16 strands in outer layer in the example). Internal resistance ( $R_c$ ) and internal reactance ( $X_L$ ) are then equal. With this formula, we obtain

$$R_c = X_L = \frac{K \sqrt{\omega \mu \rho_c}}{\sqrt{2} r \pi (2+n)} \Omega/\text{km} \quad (1-11)$$

where  $\omega$  = angular frequency

$\mu$  = permeability of conductor material (H/m)

$\rho_c$  = resistivity of conductor material ( $\Omega\text{-m}$ )

$r$  = outer radius of conductor in (m)

$n$  = no. of strands in outer layer (see Fig. 2c)

$K$  = 2.25, factor due to stranding

Results for the internal impedance calculated with the above two approaches are shown in Fig. 4. At lower frequencies, where skin effect is not yet prominent, the results for tubular conductors are fairly accurate<sup>4</sup>. After a cross-over point around 130 Hz, the results from Galloway's formula are probably more reliable since that formula takes the skin effect in the individual strands of the outer layer into account. The dotted line in Fig. 4 thus indicates the predicted field measurement values. It should be noticed that line parameters of overhead lines are seldom measured as the computed results are usually sufficiently accurate.

##### 5. Output from Line Constants Program

For the transmission line of Fig. 2, there are 14 conductors, i.e. 4 conductors per bundle in each of the three phases and 2 ground wires above. Thus, initially we have a  $14 \times 14$  series impedance and a  $14 \times 14$  shunt

capacitance matrix

$$\begin{bmatrix} V_1 \\ V_2 \\ \vdots \\ V_{14} \end{bmatrix} = \begin{bmatrix} P_{1,1} & P_{1,2} & \cdots & P_{1,14} \\ P_{2,1} & P_{2,2} & \cdots & P_{2,14} \\ \vdots & \vdots & & \vdots \\ \vdots & \vdots & & \vdots \\ P_{14,1} & P_{14,2} & \cdots & P_{14,14} \end{bmatrix}_{14 \times 14} \cdot \begin{bmatrix} Q_1 \\ \vdots \\ Q_{14} \end{bmatrix} \quad (1-12)$$

and

$$\begin{bmatrix} dV_1/dx \\ dV_2/dx \\ \vdots \\ dV_{14}/dx \end{bmatrix} = \begin{bmatrix} Z_{1,1} & Z_{1,2} & \cdots & Z_{1,14} \\ Z_{2,1} & Z_{2,2} & \cdots & Z_{2,14} \\ \vdots & \vdots & & \vdots \\ \vdots & \vdots & & \vdots \\ Z_{14,1} & Z_{14,2} & \cdots & Z_{14,14} \end{bmatrix} \cdot \begin{bmatrix} I_1 \\ I_2 \\ \vdots \\ I_{14} \end{bmatrix} \quad (1-13)$$

These  $14 \times 14$  matrices can be reduced to the desired  $3 \times 3$  matrices by considering the bundling condition in the 3 phase bundle conductors, and the zero voltage condition in both ground wires. If we denote conductors in phase A as 1,2,3,4; phase B as 5,6,7,8; phase C as 9,10,11,12 and both ground wires as 13,14, then for ground wires 13 and 14, we have

$$\begin{aligned} -\frac{dV_{13}}{dx} &= 0 \\ -\frac{dV_{14}}{dx} &= 0 \end{aligned} \quad (1-14)$$

and

$$\begin{aligned} V_{13} &= 0 \\ V_{14} &= 0 \end{aligned} \quad (1-16)$$

and for bundling in phase A, we have

$$\begin{aligned} -\frac{dV_1}{dx} &= -\frac{dV_2}{dx} = -\frac{dV_3}{dx} = -\frac{dV_4}{dx} = -\frac{dV_A}{dx} \\ I_1 + I_2 + I_3 + I_4 &\stackrel{\approx}{=} I_A \end{aligned} \quad (1-16)$$

$$\begin{aligned} V_1 &= V_2 = V_3 = V_4 = V_A \\ Q_1 + Q_2 + Q_3 + Q_4 &\stackrel{\approx}{=} Q_A \end{aligned} \quad (1-17)$$

With eqtns (1-15) and (1-17), eqtn (1-12) can be reduced to 3 equations with the desired  $3 \times 3$  potential matrix  $[P]$ <sup>15</sup>,

$$\begin{bmatrix} V_A \\ V_B \\ V_C \end{bmatrix} \stackrel{\approx}{=} \begin{bmatrix} P_{AA} & P_{AB} & P_{AC} \\ P_{BA} & P_{BB} & P_{BC} \\ P_{CA} & P_{CB} & P_{CC} \end{bmatrix}_{3 \times 3} \begin{bmatrix} Q_A \\ Q_B \\ Q_C \end{bmatrix} \quad (1-18)$$

The  $3 \times 3$  shunt capacitance matrix  $[C]$  is then obtained by simple matrix inversion  $[C]_{3 \times 3} = [P]_{3 \times 3}^{-1}$ . Similarly, eqtns (1-14) and (1-16) can be used to reduce eqtn (1-13) to 3 equations with the desired  $3 \times 3$  series impedance matrix  $[Z]$ .

$$\begin{bmatrix} dV_A/dx \\ dV_B/dx \\ dV_C/dx \end{bmatrix} = \begin{bmatrix} Z_{AA} & Z_{AB} & Z_{AC} \\ Z_{BA} & Z_{BB} & Z_{BC} \\ Z_{CA} & Z_{CB} & Z_{CC} \end{bmatrix}_{3 \times 3} \begin{bmatrix} I_A \\ I_B \\ I_C \end{bmatrix} \quad (1-19)$$

Thus, with Carson's formula and with one of the two skin effect formulae for conductors, followed by matrix reduction for bundling and ground wires, we obtain the  $3 \times 3$  series impedance and  $3 \times 3$  shunt capacitance matrices for the three phases.

The  $3 \times 3$  shunt capacitance matrix obtained from the tower geometry of the test example is shown in Table 2. the elements of the  $3 \times 3$  symmetric

series impedance matrix are shown as a function of frequency in Figs. 5 and 6. Note that the differences between both skin effect formulae hardly show up at high frequencies on a logarithmic scale.

TABLE 2.

## Capacitance Matrix of Three Phase Test Line

$$[C] = \begin{bmatrix} 0.06889 & -0.01183 & -0.00347 \\ -0.01183 & 0.07080 & -0.01183 \\ -0.00347 & -0.01183 & 0.06889 \end{bmatrix} \mu\text{F}/\text{km}$$

Elements of the resistance matrix of the test line,  
with Galloway's formula and the formula for tubular  
conductor, for skin effect

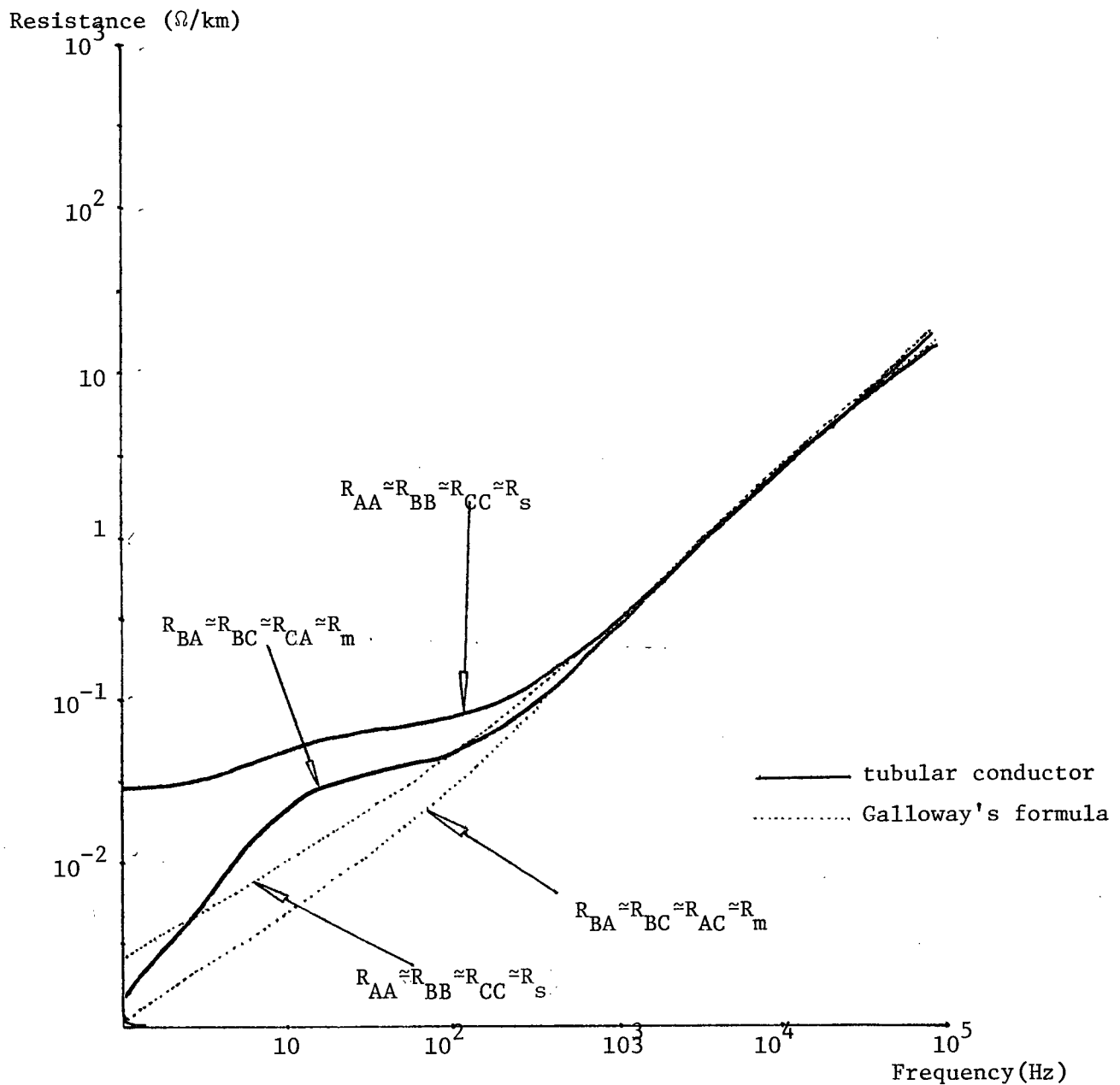


Fig.5

Elements of the reactance matrix of the test line,  
with Galloway's formula and the formula for tubular  
conductor, for skin effect

Reactance  $\omega L (\Omega/\text{km})$

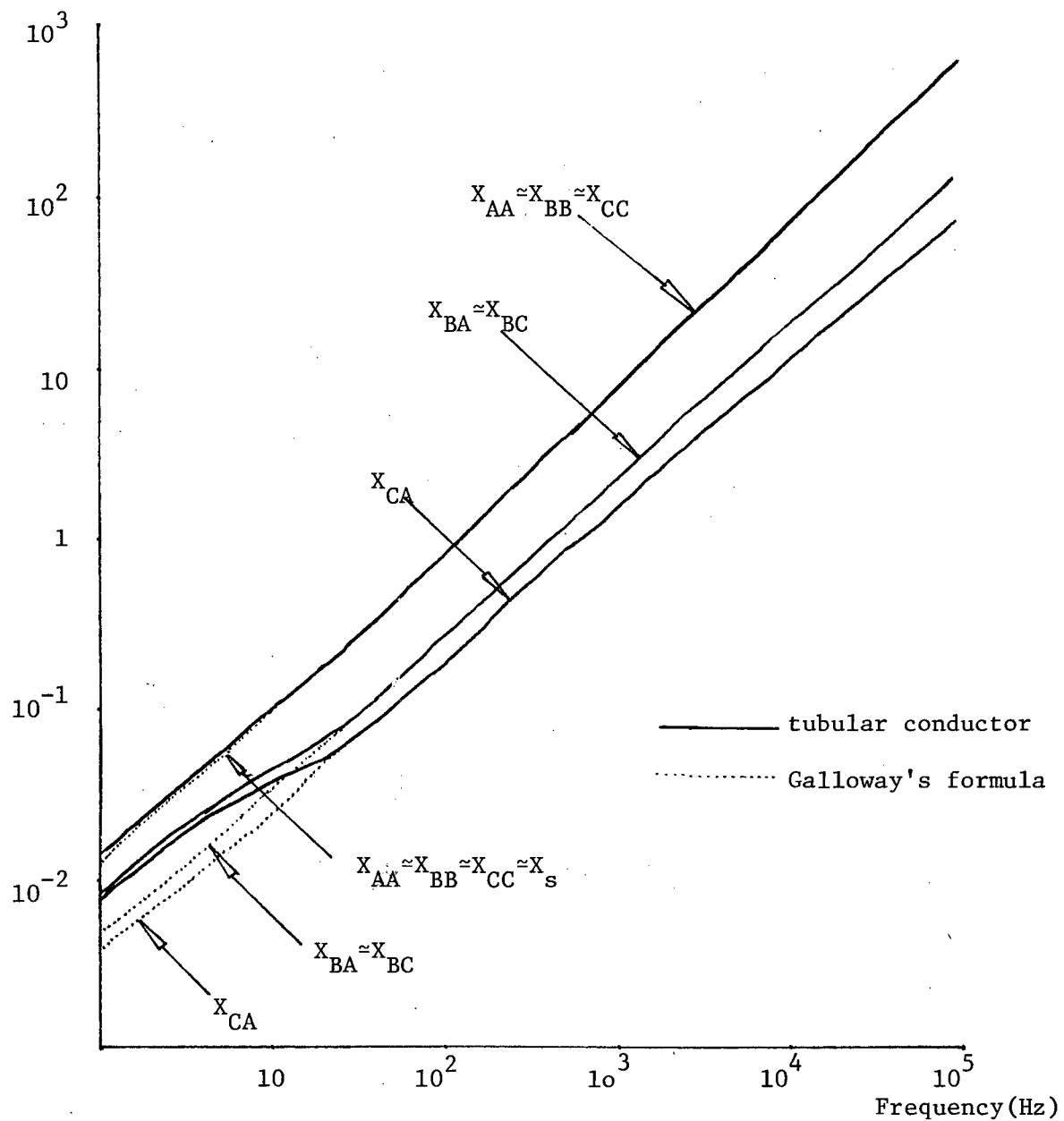


Fig.6

## 6. Positive and Zero Sequence Parameters

There are 3 modes of TEM propagation on the 3 phase test line. Each mode is decoupled from the other and has its own individual characteristics impedance and propagation constant (see later eqtn (2-8)). If the test line was transposed, which it is not, then two of the 3 modes would be characterized by positive sequence parameters while the third one would be characterized by zero sequence parameters. Thus, by idealizing the given untransposed line to a transposed one, we can look at the positive and zero sequence parameters, which will give us some insight into the overall effect of both approaches for conductor skin effect calculation (tubular conductor formula and Galloway's formula).

For the transposed line, the formulae relating position and zero sequence impedances ( $Z_{\text{pos}}$  and  $Z_{\text{zero}}$ ) to the series impedance matrix elements are given by<sup>14</sup>

$$Z_{\text{pos}} = Z_s - Z_m \quad (1-20)$$

$$Z_{\text{zero}} = Z_s + 2Z_m \quad (1-21)$$

where  $Z_s$  and  $Z_m$  are the self and mutual impedances, which in turn are the averages of the diagonal and off-diagonal elements respectively,

$$Z_s = 1/3(Z_{AA} + Z_{BB} + Z_{CC}) \quad (1-22)$$

$$Z_m = 1/3(Z_{AB} + Z_{BC} + Z_{CA}) \quad (1-23)$$

where  $Z_{ij}$  is an element of  $[Z]_{3 \times 3}$

The impedances  $Z_{ij}$  in eqtns (1-16) and (1-17) are the series impedances matrix elements shown in Figs. 5 and 6. The positive and zero sequence resistances are shown in Fig. 7. In Fig. 7, the resistance of the bundle conductor obtained with the tubular conductor formula and Galloway's

Change in sequence resistance due to change in conductor bundle resistance

Resistance ( $\Omega/\text{km}$ )

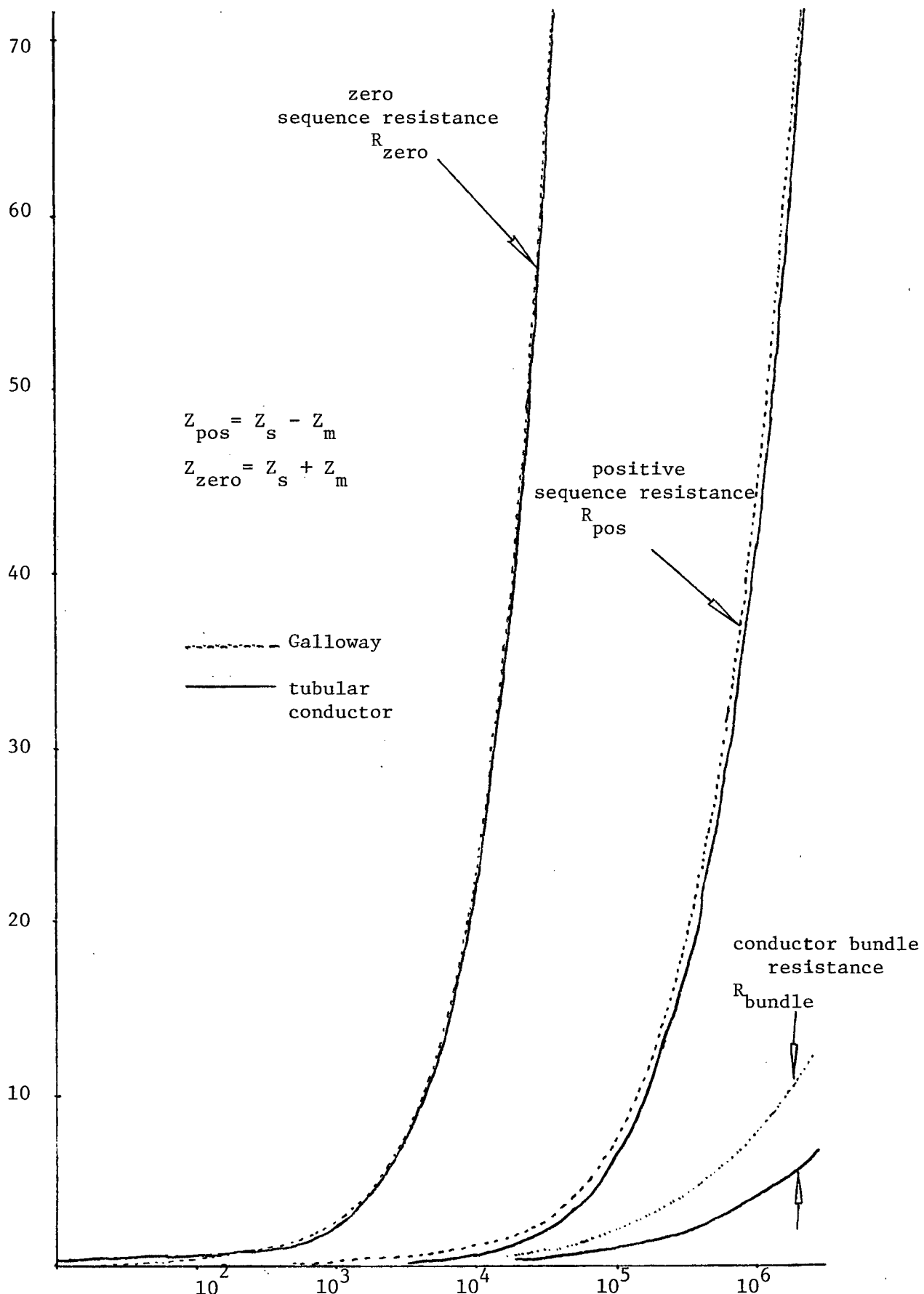


Fig. 7

formula are also shown for comparison. At higher frequencies, the conductor resistance from Galloway's formula is about twice as high ,(see also Fig. 4) as the value from the tubular conductor formula. The increase in conductor resistance ( $\Delta R_c$ ) shows up with the same value as an increase in positive sequence resistance ( $\Delta R_{pos}$ ). However, the differences in conductor resistance between the two formulae do not show up with exactly the same value in the zero sequence resistance. The difference in zero sequence resistance ( $\Delta R_{zero}$ ) is slightly higher (e.g. 9% higher at 50 KHz) due to the additional effect of the 2 eliminated ground wires. Also note that the zero sequence resistance is much higher than the positive sequence resistance. At 50 KHz, the increase in the positive sequence resistance caused by the difference in skin effect formulae is about 17% whereas the increase in the zero sequence resistance is only about 1%.

## CHAPTER II

### COMPUTATION OF TRANSFER FUNCTION FOR FREQUENCY RESPONSE OF TEST LINE

#### 1. Introduction

After knowing the series impedance matrix  $[Z_{ij}]_{3 \times 3}$  and the shunt admittance matrix with zero conductance

$$[Y_{ij}]_{3 \times 3} = j\omega [C_{ij}]_{3 \times 3}$$

of the 3-phase test line, the transfer function between the input on one phase at the sending end and the output on any one of the three phases at the receiving end can be found. For the chosen test example, one phase, designated A, is energised (see Fig. 8).

The output voltage in the 3-phase at the receiving end of the 83.212 km long test line was to be found for a period of time during which the waves reflected at the receiving end have not yet returned back from the sending end. That is, the period of investigation time  $t$  is

$$\tau < t < 3\tau$$

where  $\tau$  is the travel time of the mode with highest wave velocity.

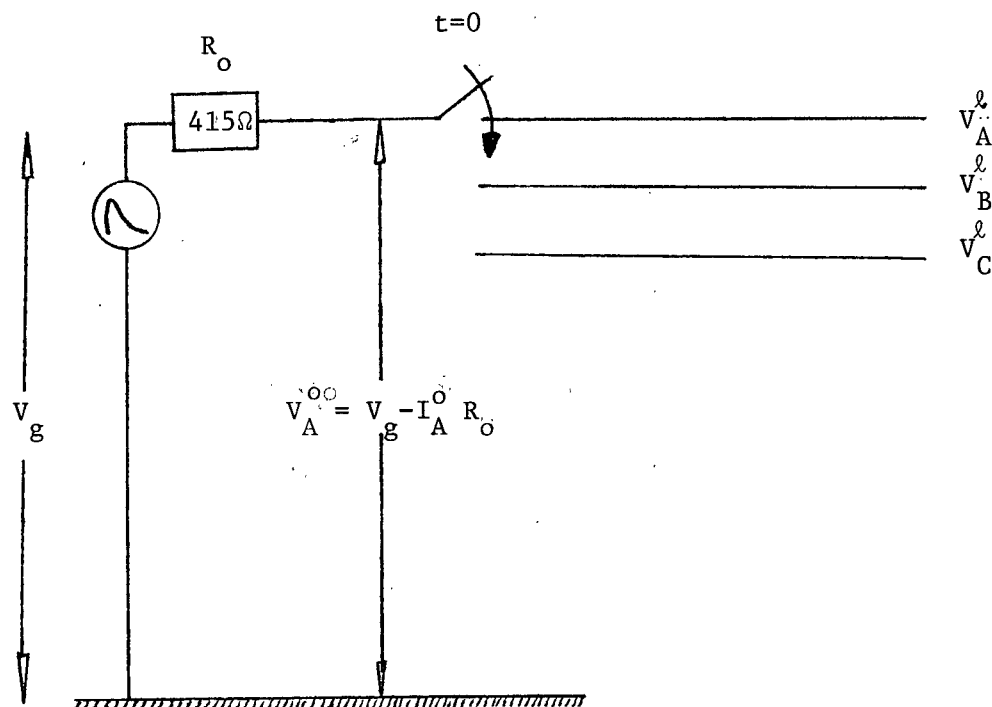
The Transfer Function Program which performs the necessary calculations is an expanded version of a program written by K.K. Tse<sup>16</sup> for a term project in EE 553 on the frequency response of B.C. Hydro's Mica Dam transmission line (see Appendix 1 for program listings).

#### 2. Outline of the theory used in the Transfer Function Program

Propagation of waves on multiphase line with constant parameters is described by the well-known general transmission line equation<sup>17,18</sup>.

$$-\left[\frac{\partial v}{\partial x}\right] = [L] \left[\frac{\partial i}{\partial t}\right]' + [R] [i] \quad (2.1)$$

$$-\left[\frac{\partial i}{\partial x}\right] = [C] \left[\frac{\partial v}{\partial t}\right] + [G] [v] \quad (2.2)$$



Boundary conditions in frequency domain

At sending end

$$V_A^O = V_g - I_A^O R_o$$

$$I_A^O \neq 0, \quad I_B^O = I_C^O = 0$$

At receiving end --- Single input triple output system

$$V_j^l = H_j(\omega) V_g; \quad j = A, B \text{ or } C$$

Fig. 8 Transmission line configurations with boundary conditions

where [v] is the 3x1 column matrix of phase voltages  
 [i] is the 3x1 column matrix of phase currents  
 [L] is the 3x3 inductance matrix  
 [R] is the 3x3 resistance matrix  
 [C] is the 3x3 capacitance matrix  
 [G] is the 3x3 conductance matrix

(N.B For overhead transmission lines, [G] is very small and is practically always neglected).

However, the above eqtns (2-1) and (2-2) are not useable for lines with frequency dependent line parameters. Instead, we have to use equations in the form of steady state phasor equations in the frequency domain

$$-\left[\frac{\partial V}{\partial x}\right] = [Z] [I] \quad (2-3)$$

$$-\left[\frac{\partial I}{\partial x}\right] = [Y] [V] \quad (2-4)$$

where  $[Z] = [R] + j\omega[L]$   
 = series impedance matrix in  $\Omega/\text{km}$  as obtained numerically from Chapter 1.

$$[Y] = j\omega[C] \quad \text{= shunt capacitance matrix in } \Omega/\text{km also from Chapter 1}$$

[V] and [I] are the vectors of phase voltages and phase currents, respectively, in the form of phasor values.

Eqtn (2-3) can be differentiated w.r.t.x to get<sup>18</sup>

$$\begin{aligned} \left[\frac{d^2V}{dx^2}\right] &= -[Z] \left[\frac{d}{dx}I\right] \\ &= [Z] [Y] [V] \\ &\triangleq [ZY] [V] \end{aligned} \quad (2-5)$$

where  $[ZY] \triangleq [Z] [Y]$

The 3x3 matrix in eqtn (2-5) has non-zero off-diagonal elements i.e. there is coupling between the phases. The easiest way to solve these coupled equations is to decouple them by modal analysis<sup>18,16</sup>. With this approach,  $[ZY]$  is transformed to a diagonal matrix with<sup>19</sup>  $[M]$ ,

$$[M]^{-1} [ZY] \cdot [M] = [\Lambda] \quad (2-6)$$

where  $[\Lambda]$  = diagonal matrix

$[M]$  = modal matrix, i.e. columns of eigenvectors of  $[ZY]$

and  $[M]^{-1}$  = inverse of  $[M]$

Both  $[M]$  and  $[M]^{-1}$  were obtained with subroutines from the UBC Computing Centre Programme Library, namely with 'DCEIGN' and 'CDINVT'<sup>20</sup>. 'DCEIGN' computes the eigenvalues and eigenvectors of the complex matrix  $[ZY]$ , and 'CDINVT' computes the inverse of the modal matrix  $[M]$ . 'DCEIGN' was tested for accuracy by running a test example with known answers<sup>19</sup>. The results agreed up to 7 significant digits. With  $[M]^{-1}$  known, the phase to mode voltage transformation is described by

$$[V^{\text{mode}}] = [M]^{-1} [V] \quad (2-7)$$

Pre-multiplying eqtn (2-5) with  $[M]^{-1}$  gives

$$[M]^{-1} \left[ \frac{d^2 V}{dx^2} \right] = [M]^{-1} [ZY] [V]$$

or  $\left[ \frac{d^2}{dx^2} V^{\text{mode}} \right] = [M]^{-1} [ZY] [V]$

$$= [M]^{-1} [ZY] [M] [V^{\text{mode}}] \quad \text{from eqtn (2-7)}$$

$$= [\Lambda] [V^{\text{mode}}] \quad \text{from eqtn (2-6)}$$

Thus, 3 second order differential equations are obtained, each decoupled from the other, namely,

$$\begin{bmatrix} \frac{d^2 V_1^{\text{mode}}}{dx^2} \\ \frac{d^2 V_2^{\text{mode}}}{dx^2} \\ \frac{d^2 V_3^{\text{mode}}}{dx^2} \end{bmatrix} = \begin{bmatrix} \lambda_1 & 0 & 0 \\ 0 & \lambda_2 & 0 \\ 0 & 0 & \lambda_3 \end{bmatrix} \begin{bmatrix} V_1^{\text{mode}} \\ V_2^{\text{mode}} \\ V_3^{\text{mode}} \end{bmatrix} \quad (2-8)$$

where  $\lambda_1$ ,  $\lambda_2$  and  $\lambda_3$  are the 3 eigenvalues of  $[ZY]$ .

The 3 phase voltages have now been transformed into 3 modal quantities, which describe the independently decoupled modes of TEM propagation. They can be transformed back to phase voltages with the mode to phase relationship derived from equation (2-7),

$$[V] = [M][V^{\text{mode}}] \quad (2-9)$$

The general solution to the second order linear differential equation of the modal voltage components is well known<sup>22</sup> because each modal component can be treated as if it were a hypothetical single phase line.<sup>23,24,25</sup>

For distance  $x = \ell$  km away from the sending end

$$\begin{bmatrix} V_{1,\ell}^{\text{mode}} \\ V_{2,\ell}^{\text{mode}} \\ V_{3,\ell}^{\text{mode}} \end{bmatrix} = \begin{bmatrix} V_{1+}^{\text{mode}} \cdot e^{-\sqrt{\lambda}_1 \ell} + V_{1-}^{\text{mode}} \cdot e^{\sqrt{\lambda}_1 \ell} \\ V_{2+}^{\text{mode}} \cdot e^{-\sqrt{\lambda}_2 \ell} + V_{2-}^{\text{mode}} \cdot e^{\sqrt{\lambda}_2 \ell} \\ V_{3+}^{\text{mode}} \cdot e^{-\sqrt{\lambda}_3 \ell} + V_{3-}^{\text{mode}} \cdot e^{\sqrt{\lambda}_3 \ell} \end{bmatrix}$$

$$\triangleq \begin{bmatrix} V_{1+}^{\text{mode}} \cdot e^{-\gamma_1 \ell} + V_{1-}^{\text{mode}} \cdot e^{\gamma_1 \ell} \\ V_{2+}^{\text{mode}} \cdot e^{-\gamma_2 \ell} + V_{2-}^{\text{mode}} \cdot e^{\gamma_2 \ell} \\ V_{3+}^{\text{mode}} \cdot e^{-\gamma_3 \ell} + V_{3-}^{\text{mode}} \cdot e^{\gamma_3 \ell} \end{bmatrix} \quad (2-10)$$

where  $\gamma_i$  = propagation constant for steady state behaviour at specific frequency

$V_{1,2,3+}^{\text{mode}}$  = Forward modal voltage waves at  $x = 0$  of A, B and C respectively, travelling from the sending end to the receiving end.

$V_{1-,2-,3-}^{\text{mode}}$  = reflected modal voltage waves at  $x = 0$  of A, B and C respectively, travelling from the receiving end to the sending end.

If we are only interested in the attenuation and distortion of the wave front, then we can assume that the line is infinitely long. We can then neglect the backward reflected voltage wave, i.e.

$$V_{1-}^{\text{mode}} = V_{2-}^{\text{mode}} = V_{3-}^{\text{mode}} = 0$$

Eqtn (2-10) is thus reduced to

$$\begin{bmatrix} V_{1,l}^{\text{mode}} \\ V_{2,l}^{\text{mode}} \\ V_{3,l}^{\text{mode}} \end{bmatrix} = \begin{bmatrix} V_{1+}^{\text{mode}} & e^{-\gamma_1 l} \\ V_{2+}^{\text{mode}} & e^{-\gamma_2 l} \\ V_{3+}^{\text{mode}} & e^{-\gamma_3 l} \end{bmatrix} \begin{bmatrix} e^{-\gamma_1 l} & 0 & 0 \\ 0 & e^{-\gamma_2 l} & 0 \\ 0 & 0 & e^{-\gamma_3 l} \end{bmatrix} \begin{bmatrix} V_{1+}^{\text{mode}} \\ V_{2+}^{\text{mode}} \\ V_{3+}^{\text{mode}} \end{bmatrix} \quad (2-11)$$

or simply by matrix notation, we have

$$[V_l^{\text{mode}}] = e^{-[\gamma]l} \cdot [V_+^{\text{mode}}] \quad (2-12)$$

where  $[\gamma] = 3 \times 3$  diagonal matrix with diagonal elements  $\gamma_1$ ,  $\gamma_2$  and  $\gamma_3$

$e^{-[\gamma]l} = [H(\omega)]$ , transfer function matrix of the transmission system and again  $[V_+^{\text{mode}}]$  = forward voltage wave at  $x = 0$ .

(N.B. The results thus obtained are also valid for the voltage response at the receiving end of an open-ended line of finite length. For times less

than 3 times travel time, the open-ended line results are simply twice the results obtained from eqtn (2-12). This doubling effect is discussed in further detail in Chapter 4, section 1.)

From eqtn (2-12), the modal voltages at the receiving end  $[V_{\ell}^{\text{mode}}]$  can be transformed to the phase voltages by the mode to phase relationship

$$\begin{aligned}[V^{\ell}] &= [M] [V_{\ell}^{\text{mode}}] && \text{from eqtn (2-9)} \\ &= [M] e^{-[\gamma]^{\ell}} [V_+^{\text{mode}}] && \text{from eqtn (2-12)}\end{aligned}$$

Thus, we can express the phase voltages at the receiving end  $[V^1]$  in terms of phase voltages at the sending end  $[V^0]$  as

$$[V^{\ell}] = [M] e^{-[\gamma]^{\ell}} [M]^{-1} [V^0] \quad (2-13)$$

Note that from eqtn (2-13), phase voltages cannot be calculated from  $[\gamma]$  alone without  $[M]$ , i.e.

$$[V^{\ell}] \neq e^{-[\gamma]^{\ell}} [V^0]$$

### 3. Inclusion of Boundary Conditions at Sending End.

For the chosen test line case, the line was energized on phase A as shown in Fig. 8. Boundary conditions for phase voltages and currents at the sending end (distance  $x = 0$  denoted by superscript 0) are then

$$[V^0] = \begin{bmatrix} V_g^0 - I_A^0 R_0 \\ V_B^0 \\ V_C^0 \end{bmatrix} \quad (2-14)$$

and  $[I^0] = \begin{bmatrix} I_A^0 \\ 0 \\ 0 \end{bmatrix} \quad (2-15)$

Substitution of eqtn (2-3) into eqtn (2-7) differentiated w.r.t.x gives

$$\begin{aligned}
 -\left[\frac{dV_{\text{mode}}}{dx}\right] &= -[M]^{-1} \left[\frac{dV}{dx}\right] \\
 &= [M]^{-1} \cdot [Z][I^0] \\
 &\triangleq [A][I^0] \\
 &= \begin{bmatrix} A_{11} & A_{12} & A_{13} \\ A_{21} & A_{22} & A_{23} \\ A_{31} & A_{32} & A_{33} \end{bmatrix} \begin{bmatrix} I_A^0 \\ 0 \\ 0 \end{bmatrix} \\
 &= I_A^0 \cdot \begin{bmatrix} A_{11} \\ A_{21} \\ A_{31} \end{bmatrix} \tag{2-16}
 \end{aligned}$$

Again, differentiating eqtn (2-12) w.r.t.x gives

$$-\left[\frac{dV_{\text{mode}}}{dx}\right] = [\gamma] e^{-x[\gamma]} [V_o^{\text{mode}}] \tag{2-17}$$

Equating R.H.S. of eqtn (2-16) and (2-17), we get

$$[\gamma] e^{-x[\gamma]} [V_o^{\text{mode}}] = I_A^0 \cdot \begin{bmatrix} A_{11} \\ A_{21} \\ A_{31} \end{bmatrix} \tag{2-18}$$

However, at the sending end we have  $x = 0$  as boundary condition, eqtn (2-18) therefore gives

$$\begin{aligned}
 [V_+^{\text{mode}}] &= [\gamma]^{-1} I_A^0 \begin{bmatrix} A_{11} \\ A_{21} \\ A_{31} \end{bmatrix} \\
 \text{or } [V_+^{\text{mode}}] &= I_A^0 \begin{bmatrix} \frac{1}{\gamma_1} & 0 & 0 \\ 0 & \frac{1}{\gamma_2} & 0 \\ 0 & 0 & \frac{1}{\gamma_3} \end{bmatrix} \begin{bmatrix} A_{11} \\ A_{21} \\ A_{31} \end{bmatrix} = I_A^0 \begin{bmatrix} A_{11}/\gamma_1 \\ A_{21}/\gamma_2 \\ A_{31}/\gamma_3 \end{bmatrix} \tag{2-19}
 \end{aligned}$$

From the phase-mode relationship of eqtn (2-9) we get the sending end phase voltage  $[V^o]$  as

$$\begin{aligned}
 [V^o] &= [M][V_+^{\text{mode}}] \\
 &= I_A^o \begin{bmatrix} M_{11} & M_{12} & M_{13} \\ M_{21} & M_{22} & M_{23} \\ M_{31} & M_{32} & M_{33} \end{bmatrix} \begin{bmatrix} A_{11}/\gamma_1 \\ A_{21}/\gamma_2 \\ A_{31}/\gamma_3 \end{bmatrix} \\
 &= \begin{bmatrix} V_A^o \\ V_B^o \\ V_C^o \end{bmatrix} \\
 &= \begin{bmatrix} V_g - I_A^o R_o \\ V_B^o \\ V_C^o \end{bmatrix} \tag{2-20}
 \end{aligned}$$

(For a detailed picture of the boundary conditions, see Fig. 8).

Now, we can evaluate the first row of eqtn (2-20).

$$V_g - I_A^o R_o = I_A^o (M_{11} A_{11}/\gamma_1 + M_{12} A_{21}/\gamma_2 + M_{13} A_{31}/\gamma_3).$$

Then, we can get the sending end current in phase A as

$$I_A^o = \frac{V_g}{M_{11} A_{11}/\gamma_1 + M_{12} A_{21}/\gamma_2 + M_{13} A_{31}/\gamma_3 + R_o} = \frac{V_g}{Z_{\text{eq}}} \tag{2-21}$$

$$\text{where } Z_{\text{eq}} = M_{11} A_{11}/\gamma_1 + M_{12} A_{21}/\gamma_2 + M_{13} A_{31}/\gamma_3 + R_o \tag{2-22}$$

Thus, substituting eqtn (2-21) into eqtn (2-19) for  $I_A^o$ , the modal voltages at the sending end are obtained as

$$[V_+^{\text{mode}}] = \frac{V_g}{Z_{\text{eq}}} \cdot \begin{bmatrix} A_{11}/\gamma_1 \\ A_{21}/\gamma_2 \\ A_{31}/\gamma_3 \end{bmatrix} \tag{2-23}$$

Using the mode-phase relationship of eqtn (2-9) again, we obtain the sending end ( $x=0$ ) phase voltages in the 3 phase as

$$\begin{bmatrix} V_A^0 \\ V_B^0 \\ V_C^0 \end{bmatrix} = \frac{V_g}{Z_{eq}} [M] \begin{bmatrix} A_{11}/\gamma_1 \\ A_{21}/\gamma_2 \\ A_{31}/\gamma_3 \end{bmatrix} \quad (2-24)$$

Also, for the receiving end at  $x = l$ , the modal voltage components are

$$\begin{aligned} [V_l^{\text{mode}}] &= e^{-l[\gamma]} [V_+^{\text{mode}}] && \text{from eqtn (2-12)} \\ &= \frac{V_g}{Z_{eq}} \begin{bmatrix} e^{-\gamma_1 l} A_{11}/\gamma_1 \\ e^{-\gamma_2 l} A_{21}/\gamma_2 \\ e^{-\gamma_3 l} A_{31}/\gamma_3 \end{bmatrix} \end{aligned} \quad (2-25)$$

Finally, the receiving end phase voltages in the 3 phase are

$$\begin{bmatrix} V_A^l \\ V_B^l \\ V_C^l \end{bmatrix} = \frac{V_g}{Z_{eq}} [M] \begin{bmatrix} e^{-\gamma_1 l} A_{11}/\gamma_1 \\ e^{-\gamma_2 l} A_{21}/\gamma_2 \\ e^{-\gamma_3 l} A_{31}/\gamma_3 \end{bmatrix} \quad (2-26)$$

It should be realized that if we excite phase  $k$  of the 3 phase, ( $k = A, B, \text{ or } C$ ), then the output phase voltages are

$$\begin{bmatrix} V_A^l \\ V_B^l \\ V_C^l \end{bmatrix} = \frac{V_g}{Z_{eq}} [M] \begin{bmatrix} e^{-\gamma_1 l} A_{1k}/\gamma_1 \\ e^{-\gamma_2 l} A_{2k}/\gamma_2 \\ e^{-\gamma_3 l} A_{3k}/\gamma_3 \end{bmatrix} \quad (2-27)$$

This is the formula that we use in the Fourier Transform Programme. It has an option to specify which of the 3 phases are to be energized for the test line case.

Thus, we obtain the transfer function  $[H(\omega)]$  for the test case as seen from Fig. 8.

$$[H(\omega)] = \begin{bmatrix} H_A(\omega) \\ H_B(\omega) \\ H_C(\omega) \end{bmatrix} \bar{Z} \begin{bmatrix} V_A^\ell \\ V_B^\ell \\ V_C^\ell \end{bmatrix} \frac{1}{V_g} \quad (2-28)$$

#### 4. Transfer function for test line

The magnitudes and phases of the transfer functions for the test case of Fig. 8 are plotted in Figs. 9 and 10, respectively, for both approaches used in evaluating the skin effect in the conductors. The difference between the two skin effect formulae only show up in the magnitude spectrum in the low frequency (0 - 100 Hz) region. The results coincide more or less at frequencies above 100 Hz.

The phase of the transfer function increases monotonically (as shown in Fig. 9). This can easily be explained for the single phase case<sup>9</sup> where the transfer function becomes

$$H(\omega) = e^{-\sqrt{YZ}\ell} = e^{\gamma\ell} = e^{-\ell\sqrt{(R+j\omega L)j\omega C}} \quad (2-29)$$

where  $\ell$  = length of line

(N.B. Compare with eqtn (2-12) for 3 decoupled modes). Expanding for real and imaginary parts of  $\gamma$  & using binomial expansion

$$\begin{aligned} (a + b)^{1/2} &= a^{1/2} + \frac{1}{2} a^{-1/2} b + \dots, \quad a \gg b. \\ \gamma &\equiv \sqrt{(R+j\omega L)j\omega C} = (R+j\omega L)^{1/2} \cdot (j\omega C)^{1/2}, \quad R \ll j\omega L \\ \gamma &\approx [(j\omega L)^{1/2} + \frac{R}{2}(j\omega L)^{-1/2}] \cdot (j\omega C)^{1/2} \\ &= \frac{R}{2} \left( \frac{C}{L} \right)^{1/2} + j\omega(LC)^{1/2} \triangleq \alpha + j\beta \end{aligned} \quad (2-30)$$

Thus, the magnitude and phase of the transfer function for the single phase line are respectively

$$|H(\omega)| = e^{-\alpha\ell} = e^{-\ell\frac{R}{2}\left(\frac{C}{L}\right)^{1/2}} \quad (2-31)$$

Magnitude  
of  $H(\omega)$

of  $H$

Magnitude of transfer functions with skin effect calculation by  
Galloway's formula and by tubular conductor formula

0.5

0.4

0.3

0.2

0.1

Phase A

tubular conductor  
Galloway's formula

Phase B

Phase C

10

$10^2$

$10^3$

$10^4$

$10^5$

$10^6$

$10^7$

$10^8$

Fig.9

Frequency (Hz)

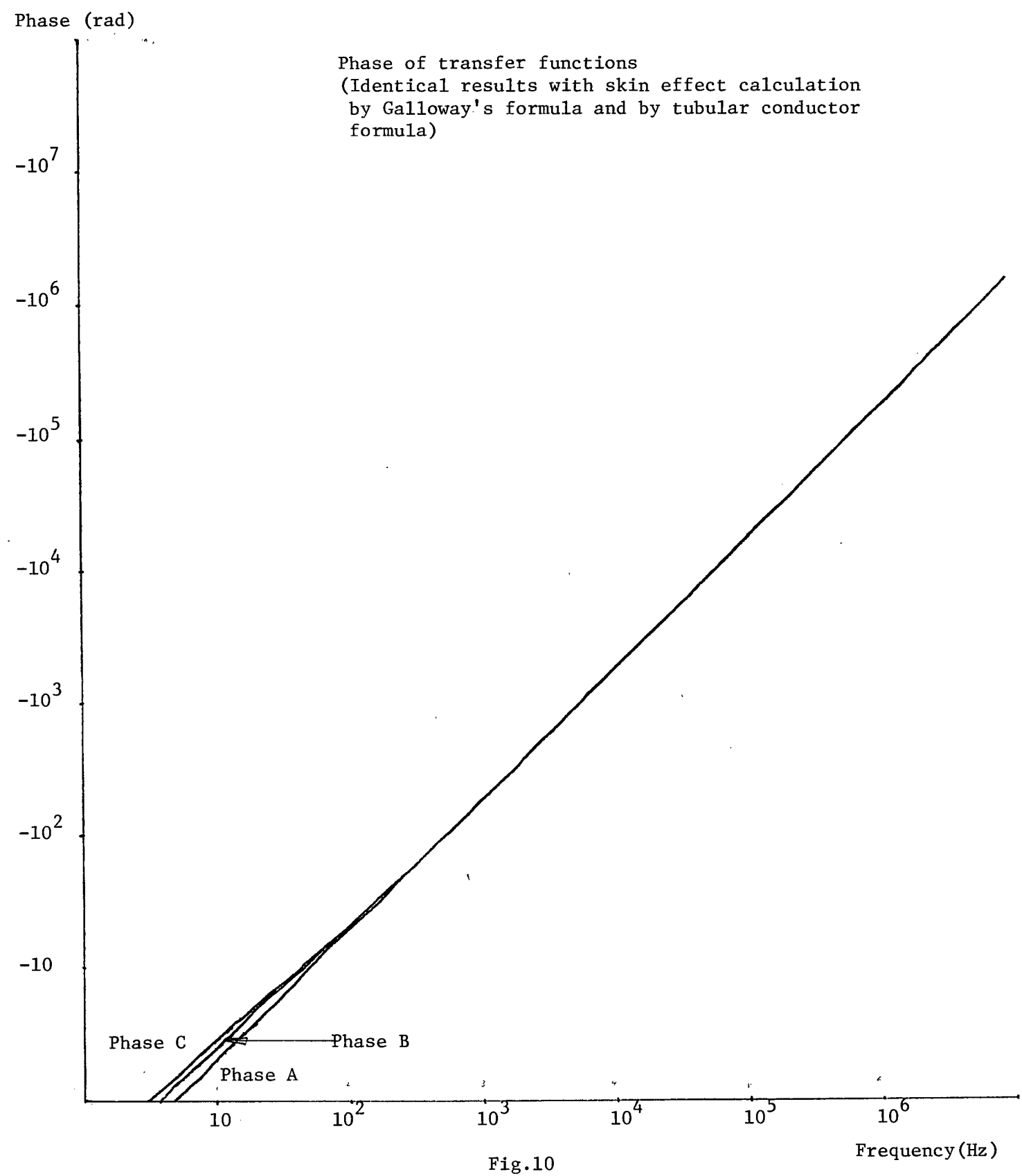


Fig.10

$$\text{and } L^H(\omega) = -\ell\beta = -\ell\omega(LC)^{1/2} \quad (2-32)$$

where  $R$  increases appreciably with frequency where  $L$  decreases slightly with frequency for zero sequence and stays more or less constant for positive sequence and where  $C$  stays constant. That is, the phase angle of the transfer function increases almost linearly with frequency, whereas the magnitude decreases with frequency similar to a low pass filter.

The calculation of angles with a FORTRAN trigonometric function statement covers only the range from  $0^\circ$  to  $360^\circ$ . Therefore, special logic to be included to extend the angles beyond  $2\pi$  (see Appendix 1 for FORTRAN listings). The separate 'PHASEPRO' program is used to guarantee that the phase angle  $\beta$  is a continuous function of  $\omega$ . This can be achieved by setting up a counter value  $k$ , where  $k$  is initially zero. Whenever the calculated phase angle falls out of the range of  $\pm\pi$  rad from the predicted extrapolated phase angle value,  $k$  will be incremented by 1

$$k := k + 1,$$

and all following phase angle values are increased by  $k(2\pi)$ . This way, the phase angle is ensured to be continuous and monotonically increasing.

## CHAPTER 3.

## TIME RESPONSE OF TEST LINE THROUGH FOURIER TRANSFORMATION

## 1. Introduction

After the frequency response of the line is known in the form of transfer functions, the output voltage can be calculated for any given input voltage ( $\bar{v}_g$ ) by Fourier Transformation. At the beginning, the input voltage  $v_g(t)$  is transformed from the time domain into the frequency domain to give  $V_g(\omega)$ . The output voltage in the frequency domain is then obtained by multiplying  $V_g(\omega)$  with the transfer function [ $H(\omega)$ ] obtained from the Transfer Function Program described in Chapter 2. i.e.

$$[V_g^l(\omega)] = [H(\omega)] V_g(\omega) \quad (3-1)$$

Finally, the inverse Fourier transformation is used to obtain the output voltages  $\bar{v}_A^l(t)$ ,  $\bar{v}_B^l(t)$  and  $\bar{v}_C^l(t)$  in the time domain. The above described techniques are applied to the test case of Fig. 8. The obtained results are then compared with the field test measurements<sup>1</sup> and with simulation results obtained by Groschupf<sup>26</sup>. The program used for the Fourier Transformations from the time to the frequency domain, and vice versa, was adopted from a version initially written by H. W. Dommel<sup>27</sup> (see Appendix 3 for program listings).

## 2. Numerical Fourier Transformation of input voltage from time to frequency

For a given input voltage  $\bar{v}_g(t)$  in the time domain, we can in general obtain the input voltage in the frequency domain  $V_g(\omega)$  with the following Fourier Transformation formula

$$A(\omega) = \int_{-\infty}^{\infty} v_g(t) \cos \omega t dt \quad (3-2)$$

$$B(\omega) = \int_{-\infty}^{\infty} v_g(t) \sin \omega t dt \quad (3-3)$$

where  $A(\omega)$  and  $B(\omega)$  are the real and imaginary parts of  $V_g(\omega)$ , respectively,

$$V_g(\omega) = A(\omega) + j B(\omega) \quad (3-4)$$

If we assume that the input voltage is zero for time  $t < 0$ , then eqtns (3-2) and (3-3) can be simplified to

$$A(\omega) = \int_0^T v_g(t) \cos \omega t dt \quad (3-5)$$

$$B(\omega) = \int_0^T v_g(t) \sin \omega t dt \quad (3-6)$$

where  $(0, T)$  is the time interval in which  $v_g(t)$  is non-zero.

#### Case 1. Input voltage defined point by point

If the input voltage is defined point by point in the integration interval  $(0, T)$  at closely spaced time intervals, then it is reasonable to assume linear interpolation between points (see Fig. 11). Then, for an interval  $(t_1, t_2)$ , we have

$$v_g(t) = v_1 + \frac{v_2 - v_1}{\Delta t}(t - t_1), \quad t_1 \leq t \leq t_2 \quad (3-7)$$

&  $\Delta t = t_2 - t_1$

Substitution of eqtn (3-7) into eqtn (3-5) gives

$$\begin{aligned} A_{12}(\omega) &= \int_{t_1}^{t_2} [v_1 + \frac{v_2 - v_1}{\Delta t}(t - t_1)] \cos \omega t dt \quad (3-8) \\ &= (v_1 - \frac{v_2 - v_1}{\Delta t}t_1) \int_{t_1}^{t_2} \cos \omega t dt + \frac{v_2 - v_1}{\Delta t} \int_{t_1}^{t_2} t \cos \omega t dt \\ &= (v_1 - \frac{v_2 - v_1}{\Delta t}t_1) \frac{1}{\omega} \sin \omega t \Big|_{t_1}^{t_2} \\ &\quad + \frac{v_2 - v_1}{\Delta t} \frac{1}{\omega} (t \sin \omega t + \frac{1}{\omega} \cos \omega t) \Big|_{t_1}^{t_2} \\ &= \frac{1}{\omega} \sin \omega t_2 [(v_1 + \frac{v_2 - v_1}{\Delta t}t_2) - \frac{v_2 - v_1}{\Delta t}t_1] \\ &\quad - \frac{\sin \omega t_1}{\omega} [(v_1 - \frac{v_2 - v_1}{\Delta t}t_1) + \frac{v_2 - v_1}{\Delta t}t_1] \\ &\quad + \frac{v_2 - v_1}{\Delta t \omega^2} (\cos \omega t_2 - \cos \omega t_1) \end{aligned}$$

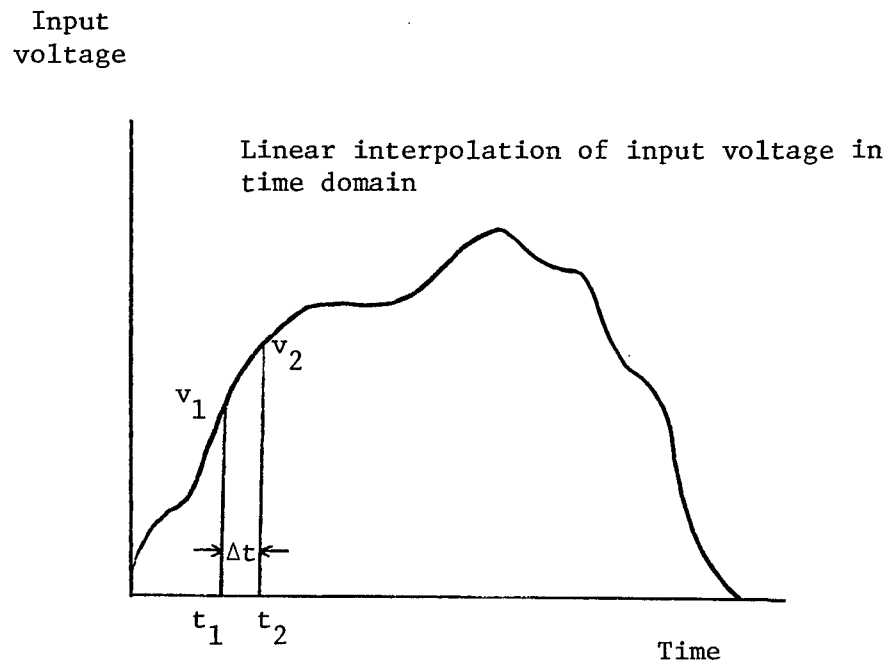


Fig.11

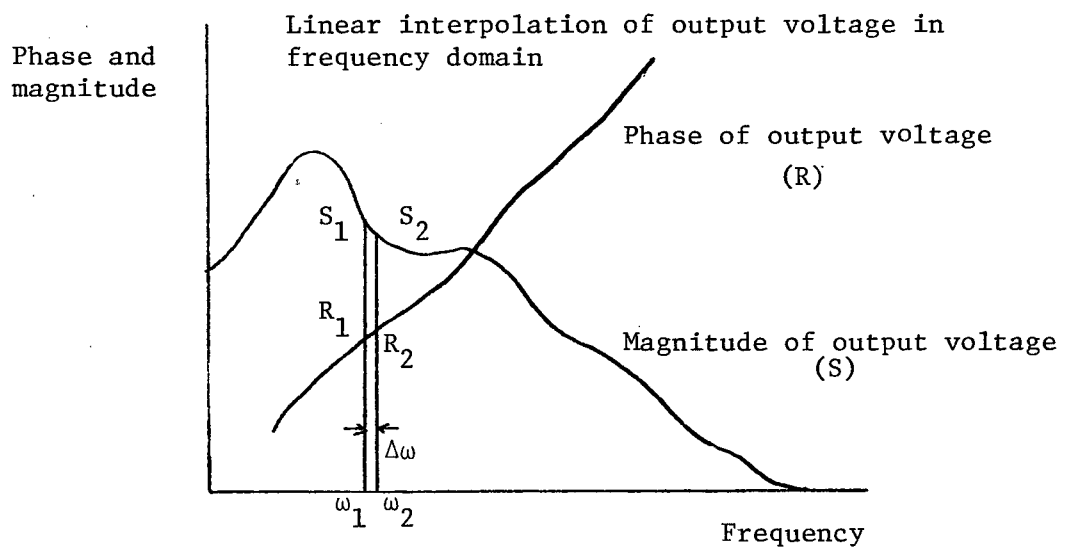


Fig.12

$$\text{or finally, } A_{12}(\omega) = \frac{1}{\omega} [v_2 \sin \omega t_2 - v_1 \sin \omega t_1 + \frac{\dot{v}_2 - \dot{v}_1}{\Delta t \omega} (\cos \omega t_2 - \cos \omega t_1)] \quad (3-9)$$

Similarly, for the imaginary voltage component in the interval  $(t_1, t_2)$ , we obtain

$$\begin{aligned} B_{12}(\omega) &= \int_{t_1}^{t_2} [v_1 + \frac{v_2 - v_1}{\Delta t} (t - t_1)] \sin \omega t \, dt \\ &= (v_1 - \frac{v_2 - v_1}{\Delta t}) \int_{t_1}^{t_2} \sin \omega t \, dt + \frac{v_2 - v_1}{\Delta t} \int_{t_1}^{t_2} t \sin \omega t \, dt \\ &= (v_1 - \frac{v_2 - v_1}{\Delta t}) \frac{1}{\omega} \cos \omega t \Big|_{t_1}^{t_2} + \frac{v_2 - v_1}{\Delta t} (-t \cos \omega t + \frac{1}{\omega} \sin \omega t) \Big|_{t_1}^{t_2}, \end{aligned}$$

$$\text{or finally } B_{12}(\omega) = \frac{1}{\omega} [-v_2 \cos \omega t_2 + v_1 \cos \omega t_1 + \frac{v_2 - v_1}{\Delta t \omega} (\sin \omega t_2 - \sin \omega t_1)] \quad (3-10)$$

The calculations of  $A_{12}(\omega)$  and  $B_{12}(\omega)$  are repeated for all time intervals to cover the whole region  $(0, T)$ . The real and imaginary part of the voltage in the frequency domain at a specific frequency  $\omega$  is then simply the sum of these parts

$$\begin{aligned} V_g(\omega) &= A(\omega) + jB(\omega) \\ &= \sum_{k=0}^N A_{k, k+1}(\omega) + jB_{k, k+1}(\omega), \text{ where } N = \frac{T}{\Delta t} \end{aligned}$$

The above calculations must be made over the entire frequency range at the same frequency points at which the transfer functions have been calculated. Output voltage in the frequency domain is thus obtained at all transfer function frequencies.

#### Case 2. Input voltage defined analytically

For some types of input voltages  $v_g(t)$ .  $A(\omega)$  and  $B(\omega)$  are known analytically<sup>28</sup>. Take a single exponential decay input voltage as an

example,

$$v_g(t) = e^{-at}, t \geq 0 \quad (3-12)$$

We can directly evaluate  $A(\omega)$  and  $B(\omega)$

$$\begin{aligned} \text{by } V_g(\omega) &= A(\omega) + jB(\omega) \\ &= \frac{1}{a+j\omega} \end{aligned} \quad (3-13)$$

Thus, we can obtain the real and imaginary voltage components in the frequency domain by the exact Fourier Transformation. With this technique, we can omit the first part of our program and obtain the output voltage in the frequency domain by multiplying eqtn (3-13) with the corresponding transfer functions, i.e.

$$[V^l] = [H(\omega)] \frac{1}{a+j\omega} \quad (3-14)$$

### 3.) Output Voltage in Frequency Domain

From eqtn (3-1), we have the output voltage in the frequency domain as

$$[V^l(\omega)] = [H(\omega)] V_g(\omega) \quad \text{from eqtn (3-1)}$$

For inverse Fourier transformation back to the time domain, (see section D), we use linear interpolation between consecutive frequency points. Thus, the output voltage frequency components must be reasonably smooth to obtain satisfactory results.

It has been shown that the magnitude of the transfer function is fairly smooth (see eqtns (2-31) and (2-32)). This is also true for the phase angle of the tranfer function provided it is extended beyond  $2\pi$  rad (see Figs. 9 and 10).

From eqtns (3-1 and (3-10)), we obtain the real and imaginary components of the input voltage. They become highly oscillating at higher frequencies and are not suitable for linear interpolation. Therefore, the

real and imaginary voltage components are converted to magnitude and phase values. The phase angle is again extended beyond  $2\pi$  by the same smoothing logic as described in Chapter 2. Thus, we can write the output voltage in the frequency domain  $V^l(\omega)$  as

$$V^l(\omega) = S(\omega) e^{j\theta} R(\omega) \quad (3-15)$$

#### 14. Output voltage in time domain by numerical inverse Fourier Transformation

From the given output voltage in the frequency domain [ $V^l(\omega)$ ], we obtain the output voltages in the time domain by inverse Fourier Transformation

$$v^l(t) = \frac{1}{\pi} \int_0^\infty V^l(\omega) e^{j\omega t} d\omega$$

From eqtn (3-15), we get

$$v^l(t) = \frac{1}{\pi} \int_0^\infty S(\omega) e^{j(\omega t + R)} d\omega \quad (3-16)$$

Similar to section B, for Fourier Transformation, the inverse Fourier Transformation also uses linear interpolation between adjacent points in the frequency domain, for the magnitudes ( $S_1, S_2$ ) of the output voltages as well as for the phase angles ( $R_1, R_2$ ). (see Fig. 12). As explained in section C, this is permissible because  $S$  and  $R$  are smooth curves in contrast to the highly oscillating real and imaginary components  $A(\omega)$  and  $B(\omega)$ . Since only a real voltage component exists in the time domain, the contribution to the output voltage from the inverse Fourier Transformation of the frequency interval  $[\omega_1, \omega_2]$  is

$$v^l(t) = \frac{1}{\pi} \int_0^\infty S(\omega) \cos(\omega t + R) d\omega,$$

or  $v_{12}^l(t) = \frac{1}{\pi} \int_{\omega_1}^{\omega_2} S(\omega) \cos(\omega t + R) d\omega \quad (3-17)$

where  $S(\omega) = S_1 + \frac{S_2 - S_1}{\Delta\omega} (\omega - \omega_1) \quad (3-18)$

$$R(\omega) = R_1 + \frac{R_2 - R_1}{\Delta\omega} (\omega - \omega_1) \quad (3-19)$$

where  $\omega_1 < \omega < \omega_2$ , &  $\Delta\omega = \omega_2 - \omega_1$

Substituting the magnitude and phase eqtns (3-18) and (3-19) into eqtn (3-13) we get

$$\begin{aligned}
 v_{12}^l(t) &= \int_{\omega_1}^{\omega_2} [S_1 + \frac{S_2 - S_1}{\Delta\omega}(\omega - \omega_1)] \cos [\omega t + R_1 + \frac{R_2 - R_1}{\Delta\omega}(\omega - \omega_1)] d\omega \\
 &= \int_{\omega_1}^{\omega_2} [(S_1 - \frac{S_2 - S_1}{\Delta\omega}\omega_1) + \frac{S_2 - S_1}{\Delta\omega}\omega] \\
 &\quad \cos [(R_1 - \frac{R_2 - R_1}{\Delta\omega}\omega_1) + (\frac{R_2 - R_1}{\Delta\omega} + t)\omega] d\omega \\
 &\stackrel{\triangle}{=} \int_{\omega_1}^{\omega_2} (a + b\omega) \cos (c + s\omega) d\omega
 \end{aligned}$$

where constants  $a, b, c$  and  $s$  are constant for a specific frequency interval,

$$a = S_1 - \frac{S_2 - S_1}{\Delta\omega} \omega_1 \quad (3-20)$$

$$b = \frac{S_2 - S_1}{\Delta\omega} \quad (3-21)$$

$$c = R_1 - \frac{R_2 - R_1}{\Delta\omega} \quad (3-22)$$

$$s = \frac{R_2 - R_1}{\Delta\omega} + t \quad (3-23)$$

Thus, we obtain

$$\begin{aligned}
 v_{12}^l(t) &= a \int_{\omega_1}^{\omega_2} \cos (c + s\omega) d\omega + b \int_{\omega_1}^{\omega_2} \omega \cos (c + s\omega) d\omega \\
 &= \frac{a}{s} \sin (c + s\omega) \Big|_{\omega_1}^{\omega_2} + \frac{b}{s} [\omega \sin (c + s\omega) + \frac{1}{s} \cos (c + s\omega)] \Big|_{\omega_1}^{\omega_2}
 \end{aligned}$$

or finally

$$\begin{aligned}
 v_{12}^l(t) &= \sin(c + s\omega_2) \left( \frac{a}{s} + \omega_2 \frac{b}{s} \right) - \sin(c + s\omega_1) \left( \frac{a}{s} + \omega_1 \frac{b}{s} \right) \\
 &\quad + \frac{b}{s} [\cos(c + s\omega_2) - \cos(c + s\omega_1)]
 \end{aligned} \quad (3-24)$$

The calculation with eqtn (3-24) is repeated for all frequency intervals to cover the frequency region over which the output voltage  $v^l(\omega)$

is defined. The output voltage at any specific time is then the sum of the contributions from all frequency interval

$$v^l(t) = \sum_{\omega=0}^{\omega'} v_{12}^l(t, \omega) \quad (3-25)$$

where  $\omega'$  is the last frequency data point.

### 5. Numerical Aspects of Fourier Transformation Program

There are several aspects which deserve special attention in the Fourier Transformation Program to ensure reasonably accurate results.

1. Suitability of linear interpolation in numerical integration - A reasonable "smoothness" of input voltage  $v_g(t)$  and output voltage in frequency domain  $V_g(\omega)$  must be guaranteed to permit linear interpolation between adjacent data points. Therefore, the magnitude and phase angle of the output voltage are used to avoid the highly oscillating real and imaginary frequency components as described in section 3.

2. Density of data points - Linear interpolation is assumed between adjacent frequency and time data points in the numerical integration loops. Too dense data points will increase computer costs drastically, while too sparse data points will result in loss of accuracy. A density of 20 points per decade in the frequency domain (on a logarithm scale) satisfies the accuracy requirement reasonably well for the test case studied. In the time domain, the density of data points for the input voltage  $v_g(t)$  depends on its wave shape and can readily be determined by the program user.

3. Number of decades in frequency domain over which  $H(\omega)$  and  $V_g(\omega)$  must be defined - It is easy to judge the required no. of decades as the transfer function magnitudes decrease substantially at high frequencies. Thus 7 to 8 decades of frequency data points, starting at  $f_{start} = 1$  Hz will

ensure reasonable accuracy without increasing computer costs too much for the test case studied. Integration between  $f = 0$  and  $f_{start}$ , where the frequency data points start is done separately, again assuming linear interpolation between 0 and  $f_{start}$ . Therefore, we can start our frequency data at any decade. This is allowable as long as the output voltage  $V^L(\omega)$  remains fairly constant and linear interpolation from zero to the starting frequency  $f_{start}$  does not cause appreciable deviations.

3. Input voltage wave form - An efficient and simple way to check the accuracy of the Fourier Transformation Program is to run it in a test mode where the transfer function is set to 1,

$$H(\omega) = 1 \ L^0$$

and to check how closely the output voltage in the time domain agrees with the input voltage  $v_g(t)$ . In our test case, the known input voltage  $v_g(t)$  is a double exponential of the form

$$v_g(t) = e^{-\alpha_1 t} - e^{-\alpha_2 t} \quad (3-26)$$

where  $\alpha_1 = 0.17 \times 10^3 \text{ s}^{-1}$

and  $\alpha_2 = 3.27 \times 10^6 \text{ s}^{-1}$

This input voltage matches exactly the output voltage thus obtained from our transformation program (see Figs. 13 and 14). In Fig. 13, in the time interval from 0 to  $7\mu\text{s}$  step widths of

$$\Delta t = 0.05\mu\text{s}$$

and  $\Delta\omega = 20 \text{ pts/decade (log scale)}$

were chosen. In Fig. 14, for time  $>10\mu\text{s}$ , the input voltage  $v_g(t)$  is essentially a single exponential  $\alpha$  decay, for which step widths of

$$\Delta t = 0.1 \text{ ms}$$

and  $\Delta\omega = 20 \text{ pts/decade (log scale)}$

were chosen.

Input voltage and calculated output voltage with  
 $H(\omega)=1.0 \angle 0^\circ$

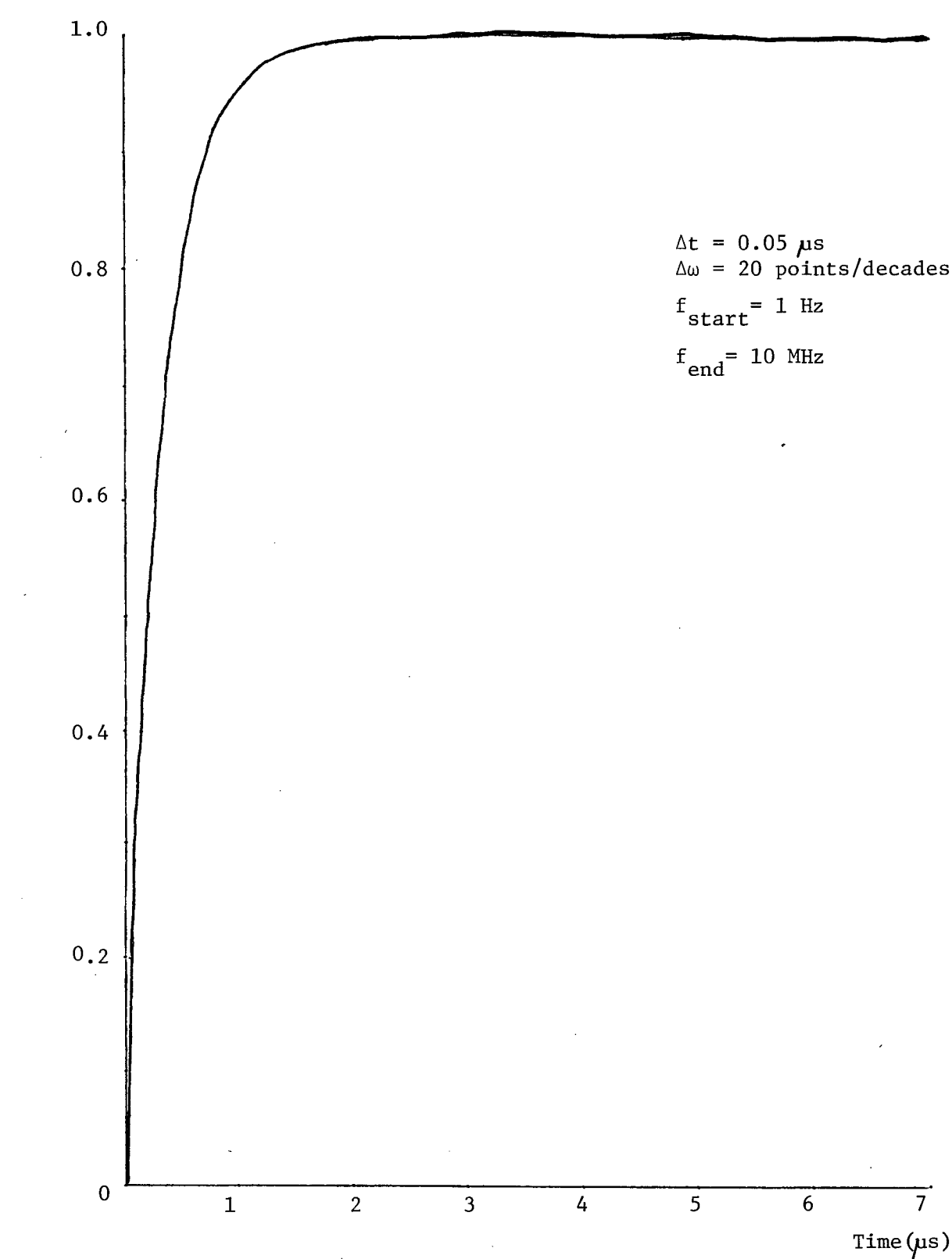


Fig.13

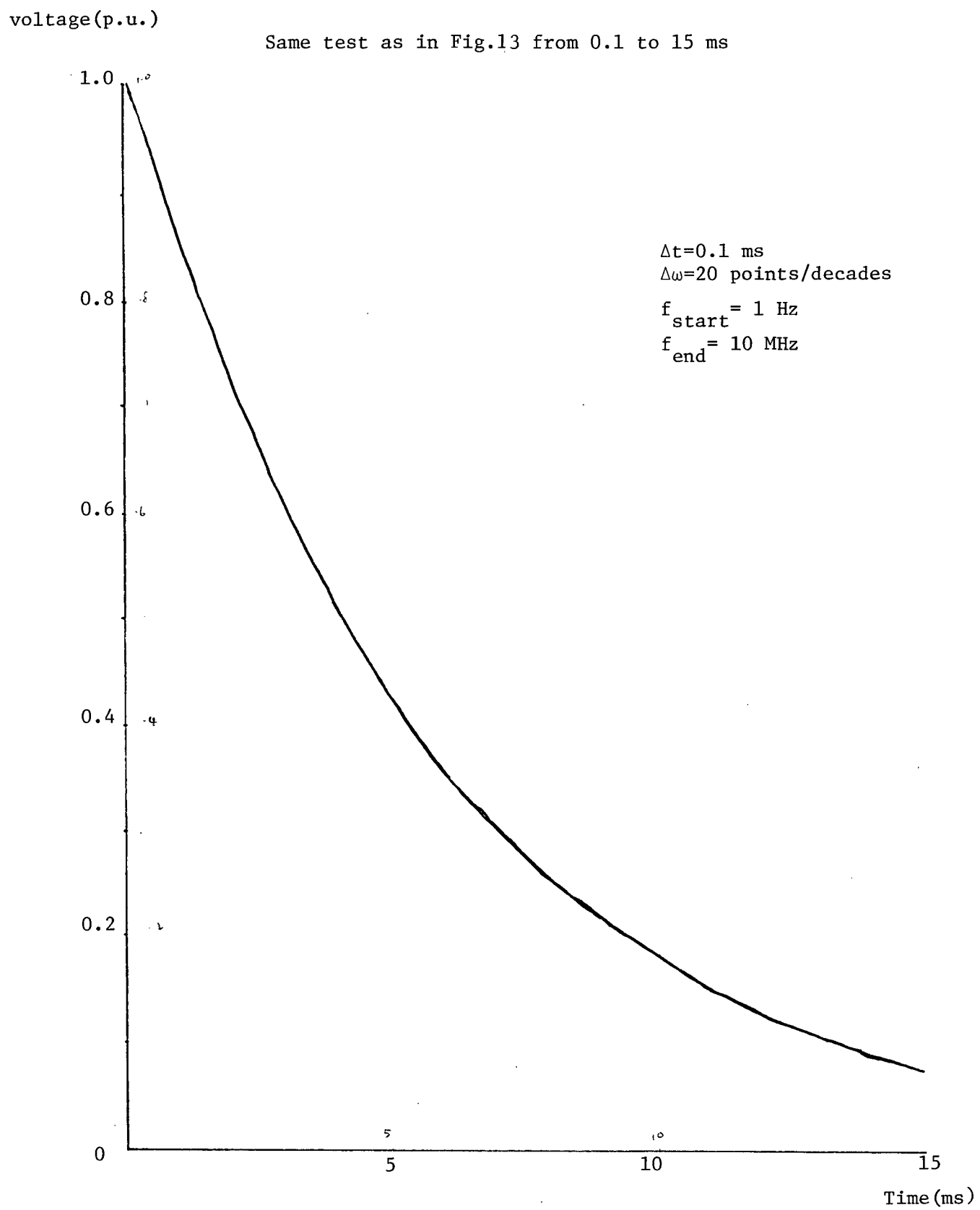


Fig.14

4. Numerical problems with step function inputs - No problem of numerical instability were encountered when the field tests of the test line were simulated. The input voltage  $v_g(t)$  in this case is a double exponential wave (see eqtn 3-26). The computations were numerically stable for large values of decay constants, namely  $\alpha_1$  and  $\alpha_2 > 10$ . However, many cases were run with step function inputs for checking purposes to debug the programme and to gain confidence before the duplication of field tests could be attempted. Serious numerical instability problems were encountered with pure step function inputs, which were then overcome by replacing the step function with an exponentially decaying function  $e^{-\alpha t}$ . The decay parameter  $\alpha$  is chosen in such a way that this function is practically equal to a step function over the time span of interest.

For an input voltage step function

$$v_g(t) = 1 \quad (3-27)$$

the voltage in the frequency domain is

$$\begin{aligned} v_g(\omega) &= \int_0^\infty 1 e^{-j\omega t} dt \\ &= \frac{-1}{j\omega} e^{-j\omega t} \Big|_0^\infty \\ &= \frac{1}{j\omega} - \frac{1}{j\omega} \lim_{t \rightarrow \infty} e^{-j\omega t} \end{aligned} \quad (3-28)$$

For time  $t \rightarrow \infty$ , the second term of eqtn (3-28) is highly oscillating and is non-zero, which causes numerical instability in the Fourier Transformation Programme. However, this problem can be remedied by introducing a slow decay into the input voltage  $v_g(t)$  as in eqtn (3-12), namely

$$v_g(t) = 1 \cdot e^{-\alpha t}, \quad t > 0 \quad \text{from eqtn (3-12)}$$

The input voltage in the frequency domain now becomes

$$\begin{aligned}
 v_g(\omega) &= \int_0^\infty e^{-\alpha t} - e^{-j\omega t} dt \\
 &= \frac{-1}{\alpha + j\omega} e^{-(\alpha + j\omega)t} \Big|_0^\infty \\
 &= \frac{1}{\alpha + j\omega} - \frac{1}{\alpha + j\omega} \lim_{t \rightarrow \infty} e^{-\alpha t} e^{-j\omega t}
 \end{aligned}$$

Now, for time to  $\infty$ , the second term is no longer oscillating due to the presence of the decay factor  $e^{-\alpha t}$  in it, and goes to zero as  $t \rightarrow \infty$ , or

$$v_g(\omega) = \frac{1}{\alpha + j\omega}$$

Furthermore, the single exponential decay voltage is better than a cut-off step function voltage (rectangular pulse) inasmuch as  $1 \cdot e^{-\alpha t}$  has a smoother amplitude and phase angle spectrum than a rectangular pulse. Thus, fewer data points per decade are required to achieve the same degree of accuracy.

The problem of numerical instability with a step function voltage is therefore easily solved by introducing the decay factor  $\alpha$ . Numerical experiments showed that  $\alpha > 10$  will be good enough to ensure numerical stability. Note that for the case  $\alpha = 10$ , the deviation of the exponentially decaying input voltage

$$v_g(t) = e^{-\alpha t}$$

from the ideal step voltage is negligible for the time span of interest here.

$$\begin{aligned}
 \text{For } t_{\max} &= 10\mu\text{s} \\
 v_g(t) &= e^{-10 \times 10^{-5}} \\
 &= 0.9999
 \end{aligned}$$

That is, the maximum deviation is less than 0.01% from the step input voltage at the upper limit  $t_{\max}$  of the study.

## CHAPTER IV

## DUPLICATION OF FIELD TESTS

## 1. Doubling effect on open-ended line.

In the analysis leading to eqtn. (2-12), we have neglected the reflected voltage wave and obtained the modal voltage for the infinite line at a distance  $\ell$  from the sending end.

$$V_{\ell}^{\text{mode}}(\omega) = V_{+}^{\text{mode}}(\omega) e^{-\gamma\ell} \quad (4-1)$$

This expression is not directly usable for the test case since we now have a transmission line of finite length which is open-ended at the receiving end terminal (see Fig. 8). The equations for the decoupled modal quantities are analogous to the equation of a single phase line, where the comparison between the infinite line and the open-ended finite line is well-known. Thus, we can use the well known solution for the single phase case for voltages and currents<sup>14,24,29</sup> in the modal domain,

$$V_o^{\text{mode}} = V_{\ell}^{\text{mode}} \cosh \gamma\ell + Z_o I_{\ell}^{\text{mode}} \sinh \gamma\ell \quad (4-2)$$

$$I_o^{\text{mode}} = \frac{V_{\ell}^{\text{mode}}}{Z_o} \sinh \gamma\ell + I_{\ell}^{\text{mode}} \cosh \gamma\ell \quad (4-3)$$

where  $I_o^{\text{mode}}$  and  $V_o^{\text{mode}}$  are the modal voltage and current at the sending end  $x = 0$ , and  $I_{\ell}^{\text{mode}}$  and  $V_{\ell}^{\text{mode}}$  are the modal voltage and current at the receiving end  $x = \ell$ .

For an open-ended line,  $I_{\ell}^{\text{mode}} = 0$ . Then we obtain from (4-2) and (4-3)

$$\begin{aligned} V_o^{\text{mode}} + Z_o I_o^{\text{mode}} &= V_{\ell}^{\text{mode}} (\cosh \gamma\ell + \sinh \gamma\ell) \\ &= V_{\ell}^{\text{mode}} e^{\gamma\ell}. \end{aligned}$$

$$\text{i.e. } V_{\ell}^{\text{mode}} = e^{-\gamma\ell} (V_o^{\text{mode}} + Z_o I_o^{\text{mode}}). \quad (4-4)$$

From  $t = 0$  to  $t < 2\tau$ , no reflection has yet come back from the receiving end, and the conditions at the sending end are therefore the same as those of an infinite line during this time period,

$$V_o^{\text{mode}} = Z_o I_o^{\text{mode}} \quad (4-5)$$

(This relationship is no longer true at the sending end after  $t \geq 2\tau$ , and is no longer true at the receiving end for  $t \geq 3\tau$ .)

With substitution of eqtn (4-5) into eqtn (4-4), we get for the receiving end,

$$V_{\ell}^{\text{mode}} = 2e^{-\gamma\ell} V_o^{\text{mode}} = 2 V_+^{\text{mode}} e^{-\gamma\ell}$$

This is twice the obtained receiving end voltage for the infinite line at location  $x = \ell$ . Thus, there is a doubling effect in the receiving end voltage of the open-ended line in comparison with the infinite line.

## 2. Comparison with field measurements and other simulation results

The output voltage at the receiving end is plotted in Fig. 15 for the test case with the voltage doubling effect taken into account. The arrival time of the first part of the voltage wave coincides closely with the time taken by electromagnetic waves (TEM propagation) in air<sup>3</sup>, i.e. 277  $\mu$ s for 83.212 km at a wave velocity of 3 km/ $\mu$ s. On a transposed line, this first part of the wave would be associated with the positive sequence parameters, and the second part of the wave would correspond to the zero sequence wave. It can be observed that the wave velocity of the zero sequence mode is slower than that of the positive sequence mode. Also the skin effect calculation with Galloway's formula gave slightly higher resistances (eg.,  $\Delta R_{\text{pos}} \approx 0.67 \Omega$  and  $\Delta R_{\text{zero}} \approx 0.73 \Omega$  at 50 KHz, see chapter 1, section E) than the formula for tubular conductors. The

output voltage based on Galloway's formula will be slightly smaller than that obtained with the tubular conductor formula. This can be seen from Fig. 15. Galloway's formula gives results closer to field measurements than the tubular conductor formula, as expected. This is because the double exponential wave front contains high frequency components where Galloway's formula is more accurate. (See Chapter 1, Sections 4 and 5).

For comparison purposes, the field measurement results from Ametani<sup>12</sup> and simulation studies by Groschupf<sup>26</sup> are included in Fig. 16. The simulation results obtained with the methods described in this thesis compare favorably with the field measurement results (within 8%). Some probable causes of discrepancies between simulation and field measurements may be due to the following phenomena:

- 1) Assumption of uniform earth resistivity ( $200 \Omega \cdot m$ ) -- An increase in earth resistivity will increase the zero sequence parameters<sup>30,31</sup> and thereby increase attenuation and decrease wave velocity of the zero sequence voltage wave. Also, a homogenous earth is only an approximation of a stratified earth which will again cause some differences in impedance line parameter calculations.
- 2) Temperature of conductor -- We assumed a conductor temperature of  $20^\circ C$ . An increase in temperature will increase conductor resistance appreciably (eg. 40% rise for increase of temperature to  $120^\circ C$ ).

However, a difference between numerical and measured values of less than 8% is well within acceptable accuracy criteria for these types of studies.

## Output voltage at receiving end of transmission line

Output voltage

(p.u.)

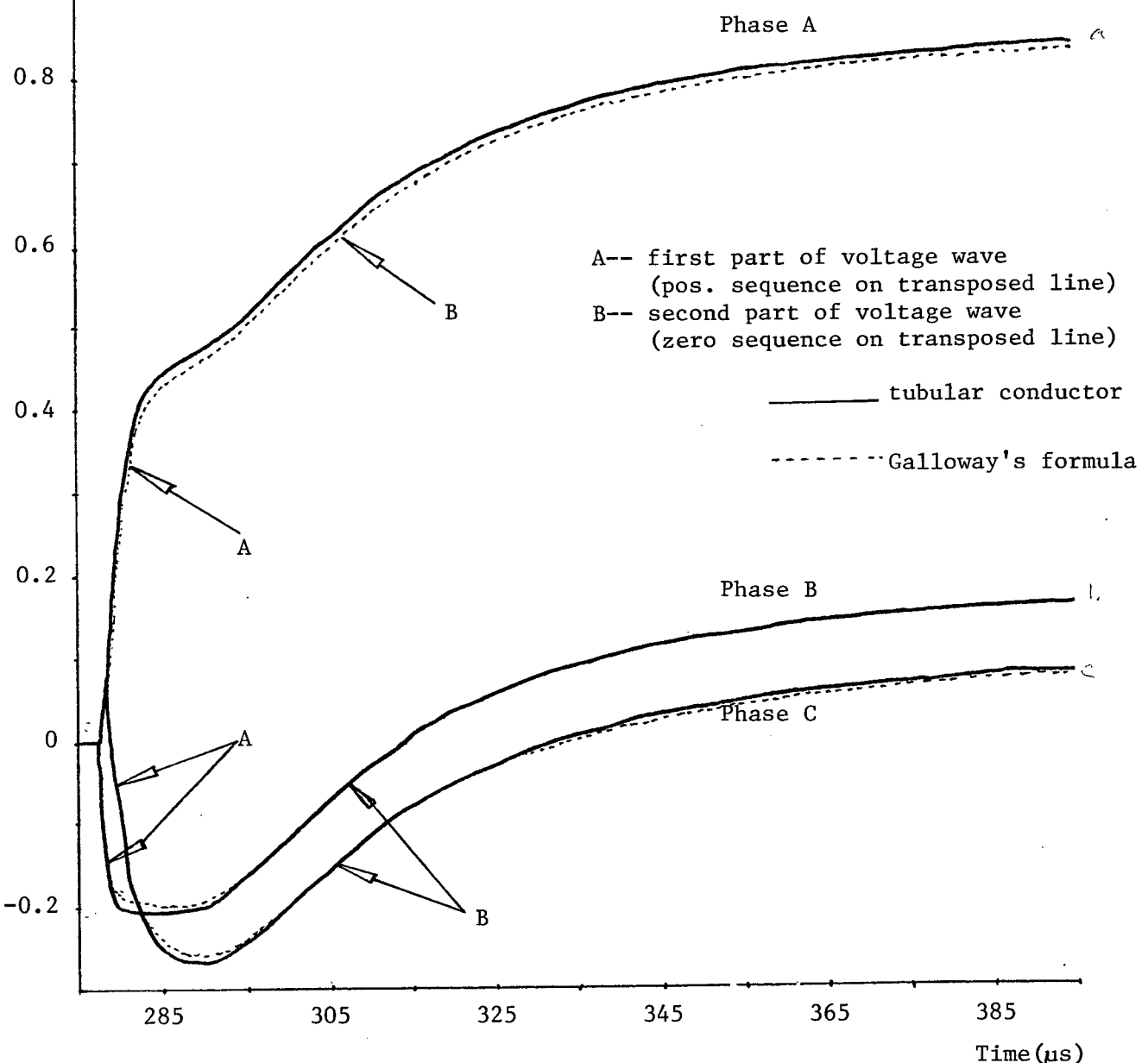
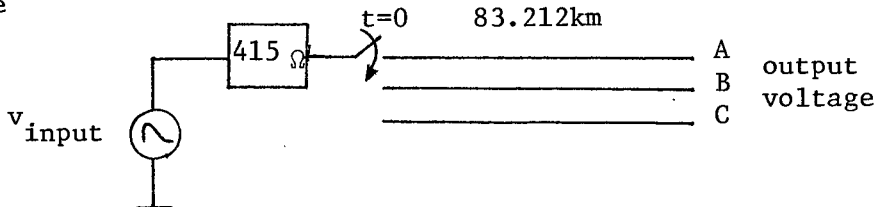


Fig.15

Output voltage at receiving end of transmission line  
with field measurement and Groschupf's simulation results

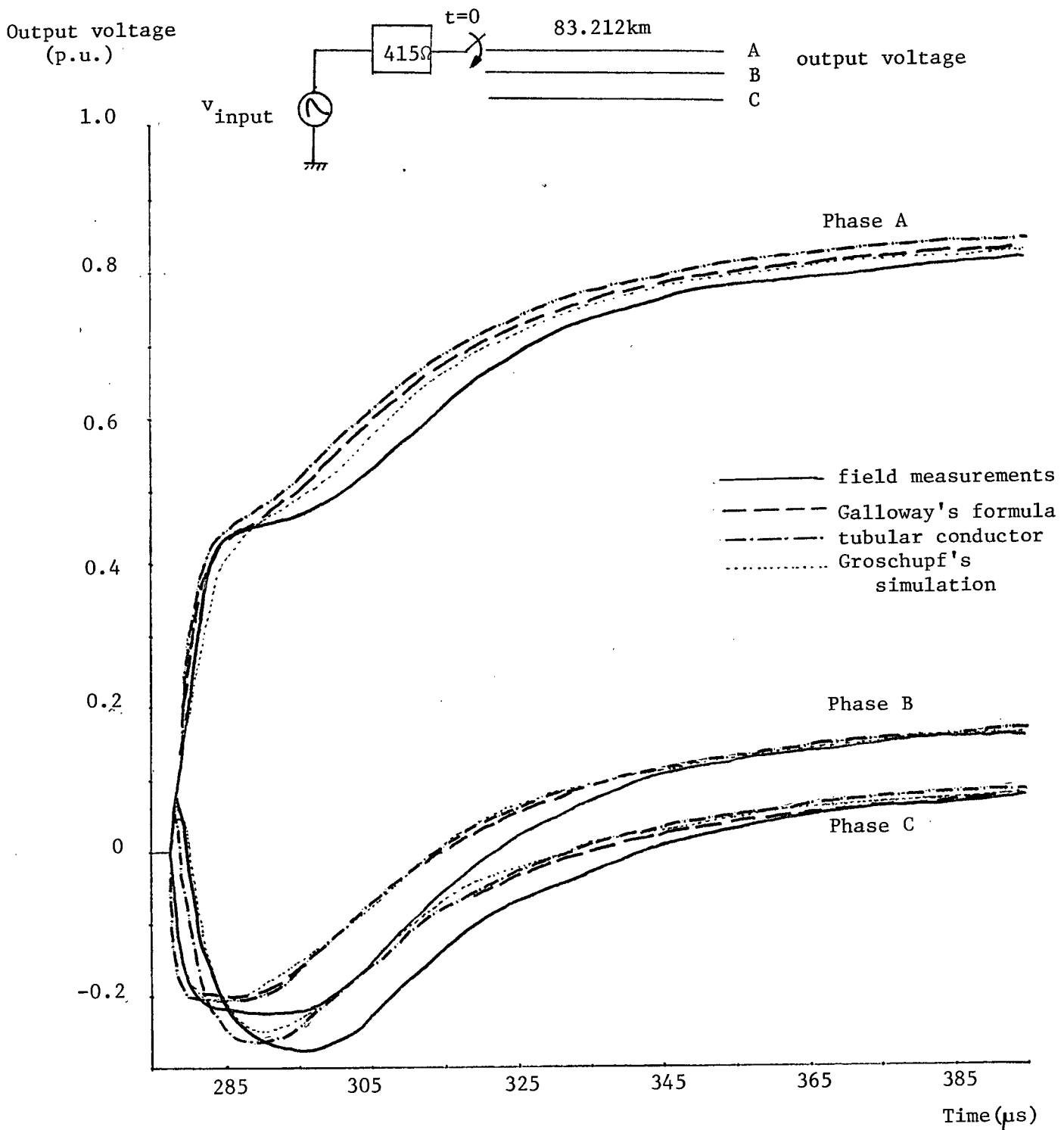


Fig.16

## CHAPTER V

## CONCLUSIONS

The attenuation and distortion of wave fronts on multiphase overhead transmission lines or underground cables was studied. A specific case of a Japanese 500 kV three-phase overhead line was chosen as a test example because field measurements were available for this line. The voltage response at the open-ended receiving end was simulated. The simulation results agreed very well with the field measurement results and with simulation results of another investigator.

Results obtained with their technique developed in this thesis will be useful for switching surge insulation co-ordination studies in power transmission systems. For instance, the technique could be used to calculate the wave front which could hit a transformer at the receiving end of the line. It should be realized, however, that this wave front would be modified by the transformer itself. This wave front modified by the transformer would be a worthwhile topic for future research. Depending on the rise time of the incident voltage wave, the transformer insulation may be more or less stressed. This is a problem of current concern in the electric utility industry<sup>32</sup>.

APPENDIX 1  
TRANSFER FUNCTION PROGRAM LISTINGS

MICHIGAN TERMINAL SYSTEM FORTPAN G(4133A)		MAIN	03-23-77	11:37:42	PAGE P001
0001	COMPLEX*16 DFT,CUND,VEXCIT			1.000	
0002	COMPLEX*16 CU(3)			2.000	
0003	COMPLEX*16 CUR1,CUR2,CURR3			3.000	
0004	COMPLEX*16 A1(3,3),B1(3,3)			4.000	
0005	REAL*8 VPF(3),ITA(IF,FREQ,TATI,VPT(3),RMAG,PHASE1,PHASE			5.000	
0006	COMPLEX*16 CZ(3,3),VO(3),VP(3),X,CURR			6.000	
0007	REAL*8 VGI,VGR,VEXRF,VEXIM,Z1(3,3),Z11(3,3)			7.000	
0008	REAL*8 FR(3),DSHRT,SUM,ONORM(3),EI(3),VR(3,3),VI(3,3)			8.000	
0009	COMPLEX*16 VP0(3,1),VP3(3,1),VM30(3,1),VM0(3,1)			9.000	
0010	COMPLEX*16 FC(3),FS(3),RU(3,3),RI(3,3)			10.000	
0011	REAL*8 A(3,3),B(3,3),C(3,3),D(3,3)			11.000	
0012	REAL*8 OMEGA,DECAY,A2+2,Z(3,3),ZI(3,3),Y(3,3)			12.000	
0013	REAL*8 M			13.000	
0014	C *** FREQUENCY INPUT = M			14.000	
0015	NE3			15.000	
0016	DELAY=10.00			16.000	
0017	RINPUT=415.			16.200	
0018	C VEXCIT IS INPUT STEP PHASE VOLTAGE			17.000	
0019	123 READ (2,3)I			18.000	
0020	3 FORMAT (E14.5)			19.000	
0021	C IMPEDANCE MATRIX Z IS COMPLEX AND ADMITTANCE MATRIX Y IS PURELY			20.000	
0022	C IMAGINARY			21.000	
0023	C *** Z X Y READ IN			22.000	
0024	READ (2,1)Y(1,1),Y(2,1),Y(2,2),Y(3,1),Y(3,2),Y(3,3)			23.000	
0025	READ (2,1)Z(1,1),Z(2,1),Z(2,2),Z(3,1),Z(3,2),Z(3,3)			24.000	
0026	1 FORMAT (E013.5)			25.000	
0027	READ (2,1)ZT(1,1),ZT(2,1),ZT(2,2),ZT(3,1),ZT(3,2),ZT(3,3)			26.000	
0028	PRINT 7			27.000	
0029	7 FORMAT (//1H1,***THE FOLLOWING ARE COMPUTING AT FREQUENCY!,E13.6			27.000	
0030	1,I -Z11			28.000	
0031	C Y(2,1)=0.			29.000	
0032	C Y(3,1)=0.			30.000	
0033	C Y(3,2)=0.			31.000	
0034	C Z(2,1)=0.			32.000	
0035	C Z(3,1)=0.			33.000	
0036	C Z(3,2)=0.			34.000	
0037	C ZI(2,1)=0.			35.000	
0038	C ZI(3,1)=0.			36.000	
0039	C ZI(3,2)=0.			37.000	
0040	C DECOUPLED CONDITION IS SET IN			38.000	
0041	IF (M.EQ.999999) GO TO 99			39.000	
0042	C			40.000	
0043	C CREATE FULL Z X Y FROM INPUT LOWER TRIANGULAR MATRIX			41.000	
0044	C			42.000	
0045	C			43.000	
0046	C			44.000	
0047	D0 10 I=1,Y			45.000	
0048	D0 10 J=1,X			46.000	
0049	Z(I,J)=Z(J,I)			47.000	
0050	Z(I,J)=ZT(J,I)			48.000	
0051	Z(I,J)=DC*OLX(Z(I,J),ZT(I,J))			49.000	
0052	Y(I,J)=Y(J,I)			50.000	
0053	10 CONTINUE			51.000	
0054	PRINT 2			52.000	
0055	2 FORMAT (/,THE REAL PART OF IMPEDANCE MATRIX Z!,/)			53.000	
0056	D0 20 I=1,N			54.000	

## MICHIGAN TERMINAL SYSTEM FORTRAN G(41336)

MAIN

03-23-77

11137842

PAGE P002

```

0037    4   FORMAT (3(SX,D13.5))
0038    PRINT 5
0039    5   FORMAT (/, 'THE IMAGINARY PART OF IMPEDANCE MATRIX Z',/)
0040    DO 30 I=1,N
0041    30   PRINT 4,(ZI(I,J) ,J=1,3)
C
C PRINTOUT OF Y
0042    PRINT 6
0043    6   FORMAT (/, 'THE SUSCEPTANCE MATRIX Y',/)
0044    DO 40 I=1,N
0045    40   PRINT 4,(Y(I,J),J=1,3)
C
C PRODUCT OF Z & Y
C
0046    DO 50 I=1,N
0047    50   DO 50 J=1,N
0048     A(I,J)=Z(I,J)
0049     B(I,J)=Y(I,J)
0050     CALL MYMULT (A,B,C,D)
0051     DO 60 I=1,N
0052     DO 60 J=1,N
0053     ZI1(I,J)=D(I,J)
0054     60   A(I,J)=ZI(I,J)
0055     CALL MYMULT (A,B,C,D)
0056     DO 70 I=1,N
0057     DO 70 J=1,N
0058     70   ZI(I,J)=D(I,J)
C
C ***** Y IS PURELY IMAGINARY
0059    PRINT 9
0060    9   FORMAT (/, 'THE REAL PART OF Z*Y MATRIX',/)
0061    DO 90 I=1,N
0062    90   PRINT 4,(ZI1(I,J),J=1,3)
0063    PRINT 8
0064    8   FORMAT (/, 'THE IMAGINARY PART OF Z*Y MATRIX',/)
0065    DO 80 I=1,N
0066    80   PRINT 4,(ZI1(I,J),J=1,3)
0067     CALL DCEIGN (Z1,ZI1,N,N,ER,EI,VR,VI,IERROR,1,0)
C
C COMPLEX EIGENVALUES ER+JEI & COMPLEX EIGENVECTORS VR+JVI
C OBTAINED FROM SUBROUTINE DCEIGN
C
0068    PRINT 11
0069    11   FORMAT (/, 'THE EIGENVALUES OF Z*Y MATRIX',/)
0070    DO 100 I=1,N
0071     EC(I)=DCMPLX(ER(I),EI(I))
0072    100  PRINT 12,ER(I),EI(I)
0073    12   FORMAT (5X,IREAL,D13.5,5X,IIMAGINARY!,D13.5)
0074    PRINT 13
0075    13   FORMAT (/, 'THE PROPAGATION CONSTANT IS THE SQUARE ROOT!',/)
0076    DO 110 I=1,N
C
C ***** PROPAGATION CONSTANT ES
0077     ES(I)=CDSQRT(EC(I))
C
C
0078    110  PRINT 12,ES(I)

```

```

MICHIGAN TERMINAL SYSTEM FORTRAN G(41336)          MAIN      03-23-77    11:37:42    PAGE 003

0079      DO 122 I=1,3
0080      SUM=0.00
0081      DO 121 J=1,3
0082      SUM=SUM+V(J,I)*V(I,J)
0083      CONTINUE
0084      ONORM=DSQRT(SUM)
0085      CONTINUE
0086      DO 120 I=1,N
0087      DO 120 J=1,N
0088      V(I,J)=V(I,J)/ONORM
0089      C MODAL TRANSFORMATION MATRIX M IS NORMALIZED
0090      RM(T,J)=DCMPLX(VR(T,J),VI(T,J))
0091      120  RM(I,J)=D(M(I,J))
0092      C MODAL MATRIX RM INVERTED TO RM1
0093      CALL CHINVT(RM1,3,3,DET,COND)
0094      DO 502 J=1,3
0095      DO 502 L=1,3
0096      A(L,J,L)=DCMPLX(0.00,0.00)
0097      DO 502 I=1,3
0098      A(I,J,L)=DCMPLX(0.00,0.00)
0099      502  A(I,J,L)=A(I,J,L)+RM(I,J,L)
0100      C ***NOTE*** EGR CHANGE FROM LINE 85 TO 92 IN ISEIS PROGRAMME 222
0101      CURR=RA(IEXCIT,2)*A(2,IEXCIT)/ES(2)
0102      CURR3=RM(IEXCIT,3)*A(3,IEXCIT)/ES(3)
0103      C IEXCIT COMPUTED FROM STEP INPUT OF TIME=20 MICROSEC, OR TAU=10 SEC
0104      C IEXCIT OBTAINED FROM FOURIER TRANSFORM FORMULA
0105      FRENEW
0106      DTAU=2.60*3.1415926535*TAU*FREQ
0107      C VEXRE=DSIN(DTAUE)/DTAU*TAU
0108      C VEXT=-(1.00*DCS(DTAUE))/DTAU*TAU
0109      C EXPONENTIAL VOLTAGE INPUT OF DECAY RATE = 'DECAY'
0110      C VOLTAGE IN FREQUENCY SPECIBUS 1/(DECAY*D(MEGA))
0111      C VEXRE=DECA*D(MEGA)*OMEGA*UMEGA
0112      C VEXT=DCPLX(VEXRE,VEXIM)
0113      C INPUT RESISTANCE BETWEEN GENERATOR & I,L IS ADDED

```

```

MICHIGAN TERMINAL SYSTEM FORTRAN G(41336)          MAIN      03-23-77    11:37:42    PAGE P004

C   IN EXPRESSION FOR CURRENT-IN-EXCITED-PHASE
C
C   CURR=EXCIT/(CURR1+CURR2+CURR3+RINPUT)
C   CURR1,CURR2,CURR3 ARE TERMS IN IN-EDNY, IN DE-ISELS,PAPER
0113
0114      DO 210 I=1,3
0115      CUR(I)=CURR*A1(I,I)*EXCIT)/ES(I)
0116
0117      C***** GET RESPONSE VOLTAGE IN 3 PHASES
0118      WRITE(*,51)
0119      S1 FORMAT(1, THE A MATRIX = M MATRIX INVERSE * PHASE IMPEDENCE MATRIX
      1)
0120      WRITE(*,131)
0121      X=(51.7037,0.0)
0122      C THIS IS DISTANCE FROM SENDING END
0123      PRINT 14
0124      14 FORMAT(1, THE FOLLOWING IS THE RESPONSE AT 30 MILES!,/)
0125      PRINT 18
0126      18 FORMAT(1,A,THE VOLTAGE IN COMPLEX FORM),)
      DO 140 I=1,N
0127      C PHASE VOLTAGE DECAY EXPONENTIALLY FROM INITIAL VOLTAGE V0
0128      C ISE'S ERROR IN ASSUMING PHASE VOLTAGE IS DECOUPLED
0129      C V01=V0*(1-EXP(-ES*I*X))
0130      C VPR(I)=REAL(VP(I))
0131      C VP(I)=DIAG(VP(I))
0132      DO 150 CONTINUE
0133      VM30=V01(1)=VM0(1,1)*C0EXP(-ES(1)*X)
0134      150 CONTINUE
0135      C PHASE VOLTAGE MATRIX VP30=M_N*VM30
      CALL CONSULT(N,M_N,VM30,VP30,3,3,1,3,3,3)
0136      C ES1=EEDEXP(-DSEAL(ES(1))*30.0D0)
0137      ES11=-DIMAG(ES(1))*30.0D0
0138      ES2=EEDEXP(-DSEAL(ES(2))*30.0D0)
0139      ES21=-DIMAG(ES(2))*30.0D0
0140      ES3=EEDEXP(-DSEAL(ES(3))*30.0D0)
0141      ES31=-DIMAG(ES(3))*30.0D0
0142      V011=EDIMAG(V01(1))
0143      V012=EDIMAG(V01(2))
0144      V013=EDIMAG(V01(3))
0145      V01RF=DREAL(VP30(1,1))
0146      VP11M=DIMAG(VP30(1,1))
0147      VP2RF=DREAL(VP30(2,1))
0148

```



## MICHIGAN TERMINAL SYSTEM: FORTRAN G(41316)

0001 SUBROUTINE MYMULT (A,B,C,D)

REAL A(3,3),B(3,3),C(3,3),D(3,3)

0002 DO 501 J=1,3

DO 501 L=1,3

0003 D(J,L)=0.

DO 501 J=1,3

C(J,L)=A(J,J)\*B(J,L)

0004 D(J,L)=D(J,L)+C(J,L)

RETURN

0005 END

0006

0007 C(J,L)=A(J,J)\*B(J,L)

0008 D(J,L)=D(J,L)+C(J,L)

0009 RETURN

0010

\*OPTIONS IN EFFECT: IN,ENDIC,SOURCE,NOLIST,NUDECK,LOAD,NOMAP

\*OPTIONS IN EFFECT: NAME = MYMULT , LINECNT = 60

\*STATISTICS\* SOURCE-STATEMENTS = 10,PROGRAM-SIZE = 620

\*STATISTICS\* NO DIAGNOSTICS GENERATED

NO ERRORS IN MYMULT

NO STATEMENTS FLAGGED IN THE ABOVE COMPILENTIONS.

## NAME NUMBER OF ERRORS/WARNINGS SEVERITY

MAIN 0 0

0

MYMULT

EXECUTION TERMINATED

0

\$2 -INDA-NWHITE 620 7-TERET-JAPAN 2-7SEDATAJAPAN

EXECUTION BEGINS

END-OF-FILE ON 7SEDATAJAPAN CAUSES A RETURN TO MTS.

EXECUTION TERMINATED

0

SL FFREIMJAPAN(1,40)

0.100000E+15 0.999845E+00 -0.643220E+04 0.896559E+01 -0.574022E+05 0.370580E+01

2 0.100000E+00 0.54561E+00 -0.56063E+01 0.4487E+00 0.63947E+02 0.106917E+00

3 0.112201E+00 0.591340E+00 -0.599751E+01 0.145424E+00 0.66161E+02 0.107401E+00

4 0.125422E+00 0.582048E+00 -0.542382E+01 0.145862E+00 0.522521E+02 0.108122E+00

5 0.141250E+00 0.582048E+00 -0.544954E+01 0.146272E+00 0.447600E+02 0.109130E+00

6 0.158489E+00 0.582039E+00 -0.531236E+01 0.146561E+00 0.361124E+02 0.109538E+00

7 0.177828E+00 0.574060E+00 -0.529400E+01 0.146822E+00 0.286725E+02 0.109538E+00

8 0.199526E+00 0.570140E+00 -0.524277E+01 0.147089E+00 0.206480E+02 0.111626E+00

9 0.223872E+00 0.566293E+00 -0.513250E+01 0.147085E+00 0.126842E+02 0.108633E+00

10 0.251149E+00 0.565524E+00 -0.509484E+01 0.147144E+00 0.640295E+02 0.105552E+00

11 0.281638E+00 0.562478E+00 -0.4966574E+01 0.147057E+00 -0.293339E+03 0.109407E+00

12 0.316228E+00 0.5555137E+00 -0.4966574E+01 0.146940E+00 -0.15273E+02 0.106185E+00

13 0.350581E+00 0.5555157E+00 -0.479459E+01 0.146755E+00 -0.179329E+02 0.1078935E+00

14 0.392107E+00 0.549644E+00 -0.440753E+01 0.146505E+00 -0.51229E+02 0.107529E+00

15 0.446664E+00 0.548612E+00 -0.461970E+01 0.146192E+00 -0.220811E+02 0.107099E+00

16 0.511124E+00 0.541017E+00 -0.533172E+01 0.1472520E+00 -0.142581E+02 0.106615E+00

17 0.562346E+00 0.537294E+00 -0.445325E+01 0.1464505E+00 -0.1516801E+02 0.106070E+00

18 0.630957E+00 0.534731E+00 -0.454539E+01 0.144624E+00 -0.512769E+02 0.105169E+00

19 0.707946E+00 0.531592E+00 -0.426553E+01 0.144339E+00 -0.570863E+02 0.10418E+00

20 0.794328E+00 0.524526E+00 -0.425573E+01 0.143832E+00 -0.6447078E+00

21 0.891251E+00 0.525538E+00 -0.408921E+01 0.143221E+00 -0.677090E+02 0.103919E+00

22 0.100000E+01 0.522622E+00 -0.402027E+01 0.142575E+00 -0.725191E+02 0.102624E+00

## APPENDIX 2

## PHASE SMOOTHING PROGRAM LISTINGS

MICHIGAN TERMINAL SYSTEM FORTRAN G(41336)		MAIN	03-23-77	11:45:13	PAGE P001
CC	PROGRAM FOURIER(INPUT,OUTPUT)			1.000	
0001	REAL*8 A(1500),PHT(1500),U(1000),FREQ,TEXT(10)			2.000	
0002	REAL*8 C2,S2,OMEGA,PHINEW,PHIOLD,H,S1,C1,FLOATN,T			3.000	
0003	REAL*8 OMDFC,STEIG,WOLD,WT,AN,AWD,BW,ANEW,AOLD,DIFF,S,AL,W1			4.000	
0004	REAL*8 TFRE(3),TFIM(3)			4.050	
0005	REAL*8 XTF(3),PTF(3)			4.200	
0006	REAL*8 DECAY,VOUT0,DT,TRISE,DTIN,POUT0			5.000	
0007	STEIG=0.00			5.200	
0008	W1=0.00			5.400	
0009	A1Z=0.00			5.600	
0010	READ(2,111)I			5.900	
0011	WRITE(6,110)I			6.200	
0012	3. CONTINUE			7.000	
0013	READ(3,33)FREQ,TFRE(1),TFIM(1),TFRE(2),TFIM(2),TFRE(3),TFIM(3)			8.000	
0014	OMEGA=6.283185307D0*FREQ			8.200	
0015	33 FORMAT(2X,E13.5,E13.5,E13.5)			9.400	
C	T=2			9.500	
0016	110 FORMAT(//10X,'PHASE EXCITED!',I3)			9.640	
0017	111 FORMAT(I3)			9.700	
C	'I' SPECIFIED WHICH PHASE TO BE SMOOTHED			10.000	
0018	AW=TFRE(I)			11.000	
0019	BW=TFIM(I)			12.000	
0020	S1=DSQRT(AW*AW+BW*BW)			14.000	
0021	S2=DARCOS(AW/S1)			15.000	
0022	IF(RW,LT.,0.,D0)-S2=6.28318530717958=S2			16.000	
0023	C1=OMEGA-W1			17.000	
0024	AKP=(STEIG*C1-S2+A1)/6.283185307			18.000	
0025	AKP=AKP+SIGN(D0,S,AKP)			19.000	
0026	KP=AKP			20.000	
0027	AKP=KP			21.000	
0028	S2=AKP*6.2831853071795800+S2			22.000	
0029	STEIG=(S2-A1)/C1			23.000	
0030	A1=E2			24.000	
0031	WRITE(6,MEGA)			25.000	
C	WRITE(7,33)HERTZ,XTF(1),PTF(1),XTF(2),PTF(2),XTF(3),PTF(3)			32.000	
0032	WRITE(7,33)FREQ,TFRE(I),TFIM(I),S1,S2			32.200	
0033	54 FORMAT(E13.5,E12.3,E15.5,E18.5,E17.5,E18.5)			33.000	
0034	GO TO 3			35.000	
0035	END			36.000	
OPTIONS IN EFFECT* ID,ESCITE,SOURCE,MOLIST,NOFILE,LOAD,NOMAP					
*OPTIONS IN-EFFECT* NAME = MAIN , LINECNT = 60					
*STATISTICS* SOURCE STATEMENTS = 35,PROGRAM SIZE = 33226					
*STATISTICS* NO-DIAGNOSTICS GENERATED					
NO ERRORS IN MAIN					
NO STATEMENTS FLAGGED IN THE ABOVE COMPILETTION.					
EXECUTION TERMINATED					
SR = LOAD 7=TFJAPAN1, 2==SOURCE* 3=TFREIMJAPAN(2) 6==SINK*					
EXECUTION BEGINS					
PHASE EXCITED 1					

## APPENDIX 3

## FOURIER TRANSFORMATION PROGRAM LISTINGS

MICHIGAN TERMINAL SYSTEM FORTRAN G(41336)		MAIN	03-23-77	12:03:25	PAGE P001
CC	PROGRAM FOURIER(INPUT,OUTPUT).			1.000	
0001	REAL,*R A(1500),PHI(1500),U(1000),FREQ(200),TEXT(10)			2.000	
0002	REAL,*R C2,S2,OMEGA,PHINEX,PHOLD,H,S1,C1,FLOATN,T			3.000	
0003	REAL,*R OMNEC,UNLD,W1,A1,A2,B1,W,A1F,W,ADL0,DIFF,S,A1,W1			4.000	
0004	REAL,*R DECAY,VOUT0,DT,TRISF,DTIN,POUT0,TFR(1500),TFIM(1500)			5.000	
0005	REAL,*R ALPHA,ALPHA1,ALPHA2,A12,V1(1000)			6.000	
0006	REAL,*R TOUT1,TARRAY(1000),DTOUT2,DTIN2			7.000	
0007	REAL,*R AJN,BIN,ITIN,TFIN,TINPUT,FLUATN			8.000	
0008	CALI FTNCMD(ISET MINUSZERO=ON!, 16)			9.000	
0009	TTTSEE=5,D=00			10.000	
0010	5 READ(2,10) KOPT,IB,IZ,OMIN,DT,TMAX,(TEXT(I),I=1,10)			11.000	
0011	IFXP=1			12.000	
0012	WRITE(6,10) KOPT,IB,IZ,OMIN,DT,TMAX			13.000	
0013	10 FORMAT(3I3,1X,3E10.3,10A4)			14.000	
0014	IF(TP,E0.0) STOP			15.000	
0015	WRITE(6,20)(TEXT(I),I=1,10)			16.000	
0016	6 FORMAT(1H0,10A4)			17.000	
0017	IWE7B*12+1			18.000	
C INPUT FOR 1/4000 MS INCIDENT WAVE				19.000	
0018	AJIN=.6800			20.000	
0019	RIN=.2700			21.000	
0020	TTTN=1.0E-6			22.000	
0021	TTTN=4000.0-D=00			23.000	
0022	ALPHA1=AJIN/TTTN			24.000	
0023	ALPHA2=RIN/TTTN			25.000	
0024	WTTF(6,800)ALPHA1,ALPHA2			26.000	
0025	800 FORMAT(1X,'INPUT VOLTAGE TIME CONSTANTS: ALPHA1=' ,E13.5,' ALPHA2=' ,E13.5)			27.000	
0026	IF(TEXP,F0.1)ALPHA=ALPHA1			28.000	
0027	IF(TEXP,F0.2)ALPHA=ALPHA2			29.000	
C CHANGE FOLLOWING TWO STATEMENTS IF DIMENSION IS CHANGED *****				30.000	
0028	WHITE(6,816)ALPHA			31.000	
0029	510 FOR IAT((//!**TIME CONSTANT IN DECAY = ',E13.5,'*****))			32.000	
0030	IF(TS.GT.1500) GO TO 97			33.000	
0031	IF(TZ.GT.2000) GO TO 97			34.000	
0032	S1=TZ			35.000	
0033	H=0.00			36.000	
0034	S2=2.3125K50929940D0/S1			37.000	
0035	DO 11 N=1,IZ			38.000	
0036	FPEA(K)=0EXP(H*S2)			39.000	
0037	11 H=N+1.DN			40.000	
C READING AMPLITUDE AND PHASE SPECTRA OR PRESETTING THEM *****				41.000	
0038	IF(KNOT,F0.1).GO TO 14			42.000	
C				42.020	
C				42.040	
C T.F. IS READ IN				42.060	
C				42.080	
C				42.100	
C				42.200	
0039	DO 12 N=2,TW			43.000	
0040	READ(3,35) A(K),PHI(K)			44.000	
C	A(K)=1.00			45.000	
C	PHI(K)=0.00			46.000	
C THIS INPUT THE TRANSFER FUNCTION EXP(-GAMMA*L) AND -BETAL				47.000	
0041	33 FORMAT(51X,2(E13.6,5X))			48.000	
0042	IF(TRBLANK(A(K)),LT.0) GO TO 200			49.000	
0043	13 FORMAT(2E10.0)			50.000	
0044	12 CONTINUE			51.000	

## MICHIGAN TERMINAL SYSTEM FORTRAN G(41336)

MAIN

03-23-77

12:03:25

PAGE P002

```

0045    18 READ(2,13)H      52,000
0046    IF(TBLANK(H).LT.0) GO TO 16   53,000
0047    GO TO 18   54,000
0048    14 DO 15 K=1,TH   55,000
0049    A(K)=1.00   56,000
0050    15 PHI(K)=0.00   57,000
0051    C READING INPUT FUNCTION *****
0052    16 H=0.00   58,000
0053    IF(KOPT.EQ.3) GO TO 24   59,000
0054    C THIS IS SKIPPED FOR OPTION 3   60,000
0055    S1=0.00   61,000
0056    C S1 IS FIRST INPUT VOLTAGE VALUE   62,000
0057    C U(1)=S1...   63,000
0058    N=1   64,000
0059    DTIN=.050-06   65,000
0060    TINPUT=DTIN   66,000
0061    WRITF(6,809)DTIN   67,000
0062    809 FORMAT(1 INPUT TIME STEP FROM 0 TO 5 MS =1,E13.4)   68,000
0063    17 IF(N.GT.200)GO TO 22   69,000
0064    FLOATIN=N   70,000
0065    TINPUT=TINPUT+DTIN   71,000
0066    TARRAYIN=TINPUT   72,000
0067    S2=(ALPHA1+ALPHA2)/(ALPHA1-ALPHA2)   73,000
0068    C ALPHA12 INPUT VOLTAGE IS SET TO POSITIVE   74,000
0069    A12=S2   74,200
0070    B19 FORMAT(1/(ALPHA1+ALPHA2)/ALPHA1-ALPHA2)= 1,E14.5)   75,000
0071    S2=S2*(DEXP(-ALPHA1*TINPUT)-DEXP(-ALPHA2*TINPUT))   76,000
0072    C INPUT VOLTAGE S2 IS PRESET INSTEAD OF READ-IN   77,000
0073    C S2=S2*DEXP(-ALPHA1*TINPUT)   78,000
0074    C S2=FLOATIN*DTIN/TRISE   79,000
0075    C N=N+1   80,000
0076    IF(KOPT.EQ.7)GO TO 97   81,000
0077    H=(S1+S2)*DTIN/2.+H   82,000
0078    S1=S2   83,000
0079    U(N)=S2   84,000
0080    N=N+1   85,000
0081    GO TO 17   86,000
0082    22 IF(N.LT.2) GO TO 95   87,000
0083    TMAXIN=TINPUT   88,000
0084    N=N+1   89,000
0085    TIN2=TMAXIN/2.   90,000
0086    WRITE(6,801)H   91,000
0087    801 FORMAT(1 TIME-VOLTAGE AREA OF INPUT = 1,E15.5)   92,000
0088    C FIRST 100 ENTRY OF INPUT VOLTAGE IS PRINTED ON   93,000
0089    C THE VOLTAGE INPUT AT ZERO FREQ IS F(w=0)=TIME OF STEP = H   94,000
0090    WRITE(6,B19A12)   95,000
0091    C WRITE(6,B19A12)   96,000
0092    WRITE(6,72) (U(I),I=1,N)   97,000
0093    C VOUTO=1.00/DECAY   98,000
0094    WRITE(6,B11)   99,000
0095    B11 FORMAT(1//TIME OF INPUT VOLTAGE!)   100,000
0096    WRITE(6,B12)(TARRAY(II),II=1,200)   101,000
0097    B12 FORMAT(10E11.3)   102,000
0098    55 FORMAT(1//OUTPUT VOLTAGE IN FREQ DOMAIN AT FREQ=0. 1,2E15.5)   103,000
0099    H=1.0/H   104,000
0100    C TRANSEFORM INPUT FUNCTION FROM TIME TO FREQUENCY DOMAIN *****   105,000
0101    24 WRITE(6,32)   106,000
0102    32 FORMAT('U',24X,'INPUT FUNCTION IN FREQUENCY DOMAIN',19X,'TRANSFER'   107,000
0103    'FUNCTION',1,FREQUENCY(HZ) REAL V  IMAGINARY AMPLITUDE(Absolute'   108,000

```

```

MICHIGAN TERMINAL SYSTEM FORTRAN G(41336)          MAIN      03-23-77    12:03:25    PAGE P003

2). PHASE(RADIANS)...AMPLITUDE(Absolute),ANGLE(RADIANS).1.3X.'OUTPUT')   109.000
STE1620.                                         110.000
W1=0.00.                                         111.000
A1=0.00.                                         112.000
0.0091                                           0.0092                                           0.0093
Q=0.0C=0MIN*.6.2831853071796D0
IP20
C PRINTOUT OF FREQUENCY...ZERO-ENTRY
C1=1.0D0
0.0094                                           C WRITE(6,54)W1,C1,H,W1,A1,PHI()
      C 1SOURCE=2
0.0095                                           0.0096                                           0.0097
      36 IP=IP+1
      IF(IP.GT.IR) GO TO 57
      K=0
      58 K=K+1
      IF(K.GT.12) GO TO 44
      OMEGAE=FREQ(K)*ACMDEF
0.0101
0.0102                                           HERTZ=OMEGA/6.2831853071796D0
0.0103                                           C1=1.0D0
0.0104                                           IF(KOPL.EQ.3) GO TO 220
      S1=0.00
      A=0.00
      R=0.00
0.0105                                           IF((KOP1.EQ.1)GO TO 815
      TOLD=1
      UOLD=0(1)
      DO 48 I=2,N
      UJ=U(I)
      T=TOLD
      T=LOLD
      C  C=OMEGA*T
      C2=0.0*EGA*TARRAY(I)
      S2=0.0*SIN(C2)
      C2=0.0*COS(C2)
      T=(U1-UOLD)/(D1*OMEGA)
      A=(C2-C1)*T+U1*S2-UOLD*S1*A
      B=U1*C2-(S2-S1)*T-UOLD*C1*R
      S1=S2
      0.0119
      0.0120                                           C1=E2
      0.0121                                           UOLD=U1
      0.0122                                           48 TOLD=1
      0.0123                                           A=SEAN/D*EGA
      0.0124                                           P=ER4/G*EGA
      0.0125                                           C
      C 815 CONTINUE
      C 4W AND RW ARE NOW OUTPUT VOLTAGE IN FREQ DOMAIN
      C READ(3,34)MERTIZ
      C
0.0126                                           C
      C 4W=12*ALPHA1*(ALPHA1+ALPHA1*OMEGA*G*EGA)
      C 4R=12*OMEGA*(ALPHA2+ALPHA2*OMEGA*G*EGA)
      C 4H=5**+A12**OMEGA/(ALPHA1+ALPHA1*OMEGA)
      C 4MEGA=6.283153071796D0*HERTZ
      C READ(3,33)AW RW
      C
0.0127                                           C
      C 4W=12*ALPHA1*(ALPHA1+ALPHA1*OMEGA*G*EGA)
      C 4R=12*OMEGA*(ALPHA2+ALPHA2*OMEGA*G*EGA)
      C 4H=5**+A12**OMEGA/(ALPHA2+ALPHA2*OMEGA)
      C 4MEGA=6.283153071796D0*HERTZ
      C
0.0128                                           C
      C 4W=12*OMEGA*(ALPHA2+ALPHA2*OMEGA*G*EGA)
      C 4R=12*OMEGA*(ALPHA1+ALPHA1*OMEGA)
      C 4H=5**+A12**OMEGA/(ALPHA1+ALPHA1*OMEGA)
      C 4MEGA=6.283153071796D0*HERTZ
      C
0.0129                                           C
      C 4W=12*OMEGA*(ALPHA2+ALPHA2*OMEGA*G*EGA)
      C 4R=12*OMEGA*(ALPHA1+ALPHA1*OMEGA)
      C 4H=5**+A12**OMEGA/(ALPHA2+ALPHA2*OMEGA)
      C 4MEGA=6.283153071796D0*HERTZ
      C
0.0130                                           C
      C 4W=12*OMEGA*(ALPHA2+ALPHA2*OMEGA*G*EGA)
      C 4R=12*OMEGA*(ALPHA1+ALPHA1*OMEGA)
      C 4H=5**+A12**OMEGA/(ALPHA1+ALPHA1*OMEGA)
      C 4MEGA=6.283153071796D0*HERTZ
      C
0.0131                                           C
      C 4W=12*OMEGA*(ALPHA2+ALPHA2*OMEGA*G*EGA)
      C 4R=12*OMEGA*(ALPHA1+ALPHA1*OMEGA)
      C 4H=5**+A12**OMEGA/(ALPHA1+ALPHA1*OMEGA)
      C 4MEGA=6.283153071796D0*HERTZ
      C
0.0132                                           C
      C 4W=12*OMEGA*(ALPHA2+ALPHA2*OMEGA*G*EGA)
      C 4R=12*OMEGA*(ALPHA1+ALPHA1*OMEGA)
      C 4H=5**+A12**OMEGA/(ALPHA1+ALPHA1*OMEGA)
      C 4MEGA=6.283153071796D0*HERTZ
      C
0.0133                                           C
      C 4W=12*OMEGA*(ALPHA2+ALPHA2*OMEGA*G*EGA)
      C 4R=12*OMEGA*(ALPHA1+ALPHA1*OMEGA)
      C 4H=5**+A12**OMEGA/(ALPHA1+ALPHA1*OMEGA)
      C 4MEGA=6.283153071796D0*HERTZ
      C

```

## MICHIGAN TERMINAL SYSTEM FORTRAN G(41336)

MAIN

03-23-77

1210325

PAGE P004

```

0134      S2=DARCOS(AW/S1)          163.000
0135      IF(RA_.LT.0.00) S2=6.28318530717958-S2    164.000
0136      C1=0MEGA-W1            165.000
0137      AKP=(STFIG*(C1-S2+A1)/6.283185307           166.000
0138      AKP=AKP+SIGN(0.5,AKP)        167.000
0139      KPF=AKP                168.000
0140      AKP=AKP                169.000
0141      S2=AKP*6.28318530717958D0+S2        170.000
0142      STETG=(S2-A1)/C1          171.000
0143      A1=S2                  172.000
0144      W1=0MEGA                173.000
0145      C1=S1/TMAXIN          174.000
C      C1=S1                  175.000
C      AMPLITUDE OF VOLTAGE OBTAINED BY FORMULA AND PROGRAMME ARE PRINTED 176.000
C      OUT AS C1 AND S1          176.000
C      53 ISTORE=ISTORE+1       177.000
C      ISTORE INCREMENTAL SHIFTED TO LINE 147          178.000
C      WRITER(6,54) HERTZ,AW,BW,S1,S2,A(ISTORE),PHI(ISTORE) 179.000
C      C. A & PHI ARE STILL TRANSFER FUNCTION AS READ IN FROM INPUT FILE 180.000
0146      XTF=A(ISTORE)          181.000
0147      PTF=PHI(ISTORE)        182.000
0148      54 FORMAT(F13.5,2F12.3,F15.5,F13.5,F17.5,F13.5,3X,2E13.5) 183.000
0149      A(ISTORE)=S1*A(ISTORE)        184.000
0150      PHT(ISTORE)=S2+PHT(ISTORE)        185.000
C      C. A & PHI NOW BECOMES OUTPUT VOLTAGE & PHASE AS AFTER #171 186.000
0151      WRITER(6,54)HERTZ,AW,BW,S1,S2,XTF,PTF,A(ISTORE),PHI(ISTORE) 187.000
0152      53 ISTORE=ISTORE+1       188.000
C      189.000
0153      GO TO 38              190.000
0154      44 OMDEC=OMDEC*10.00     191.000
0155      GO TO 36              192.000
C      TRANSFER OUTPUT FUNCTION FROM FREQUENCY TO TIME DOMAIN ***** 193.000
0156      57 CONTINUE          194.000
C      195.000
C      DTOUT IS DELTA T OF OUTPUT          196.000
0157      DTOUT=.25D0-06          197.000
0158      TOUT1=260.E-6          198.000
0159      T=TOUT1                199.000
0160      WRITE(6,58) DTOUT,T        200.000
0161      58 FORMAT(1QOUTPUT FUNCTION V2(T). DELTAT=!,F12.5,! ,INITIAL TIME = !, 201.000
1E12.5)
C      TF0=0.999803          201.000
C      201.020
C      201.050
C      201.100
C      201.150
C      201.200
C      201.250
0162      TF0=.0894522          201.300
C      TF0=.0370565          201.700
C      GALLAGWAY'S FORMULA ON 'SKIN' DECREASE T.F.          201.760
C      201.820
C      201.880
0163      A(1)=TF0*A12*(1.00/ALPHA1-1.00/ALPHA2)        202.000
0164      PHI(1)=0.00          203.000
0165      WRITE(6,55)A(1),PHI(1)        204.000
0166      KT=0                  205.000
0167      63 AW=0.00          206.000
0168      BW=0.00              207.000

```

```

MICHIGAN TERMINAL SYSTEM FORTRAN G(41336)   MAIN   03-23-77  12103125  PAGE P005

0169      K1EKT1]                                *****  

          C CHANGE FOLLOWING STATEMENT IF DIMENSION IS CHANGED *****  

          IF(K1.GT.1500) GO TO 97  

0170      S1ENDNS(PHIC1)]  

0171      C1ENDNS(PHIC1)]  

0172      C1ENDNS(PHIC1)]  

0173      IP=0  

0174      JSTOREE1  

          OMDEC=OM14*6.283185307179586  

0175      A1DNEC=A14*6.283185307179586  

0176      PHINC=PHIC1STORE]  

0177      PHINC=PHIC1STORE]  

0178      64  IP=IP+1  

0179      IF(IP.GT.18) GO TO 70  

0180      KED]  

0181      66  K=K+1  

0182      IF(K.GT.12) GO TO 68  

          OMEGAE=PIELOCK)*NDEC  

0183      ISTOREE1STOREE+1  

          PHINEW=PH1(ISTORE)  

          ANEKA(ISTORE)]  

0184      DIFF=1.D0/(OMEGAARW)  

          S=1.D0/(1.+PHINEW*PHIOLD)*DIFF)  

0185      C2=OMEGAI+PHINEW  

0186      IF(C2.GT.0.RE06)C2=C2-626318.53071795900  

0187      IF(C2.GT.0.AE06)C2=C2-626318.53071795900  

          221.000  

0188      222.000  

0189      223.000  

0190      224.000  

0191      225.000  

0192      226.000  

0193      227.000  

0194      228.000  

0195      229.000  

0196      230.000  

0197      231.000  

0198      232.000  

0199      233.000  

0200      234.000  

0201      235.000  

0202      236.000  

0203      237.000  

0204      238.000  

0205      239.000  

0206      240.000  

0207      241.000  

0208      242.000  

0209      243.000  

0210      244.000  

0211      245.000  

0212      246.000  

0213      247.000  

0214      248.000  

0215      249.000  

0216      250.000  

0217      251.000  

0218      252.000  

0219      253.000  

0220      254.000  

0221      255.000  

0222      256.000  

0223      257.000  

0224      258.000  

0225      259.000  

0226      260.000  

0227      261.000  

0228      262.000  

0229      263.000  

0230      264.000  

          100 STOP

```

## MICHIGAN TERMINAL SYSTEM FORTRAN G(41336)

MAIN

03-23-77

12:03:25

PAGE P006

0222	200 DO 210 I=K,IW	265.000
0223	A(I)=0.00	260.000
0224	210 PHI(I)=0.00	267.000
0225	GO TO 16	268.000
0226	220 S1=1.00	269.000
0227	S2=0.00	270.000
0228	GO TO 53	271.000
0229	END	272.000

\*OPTIONS IN EFFECT\* INHEDCIC,SOURCE,NOLIST,NOECK,LOAD,NOMAP

\*OPTIONS IN EFFECT\* NAME = MAIN , LINECNT = 60

\*STATISTICS\* SOURCE STATEMENTS = 229, PROGRAM SIZE = 79864

\*STATISTICS\* NO DIAGNOSTICS GENERATED

NO ERRORS IN MAIN

NO STATEMENTS FLAGGED IN THE ABOVE COMPILETTION.  
EXECUTION TERMINATED

SR -LOAD 2=\*SOURCE\* 6=\*SINK\* 7=FENDALPHA12B 3=TFJAPAN2  
EXECUTION BEGINS  
2 9 20 0.100E+00 0.500E-06 0.450E-03

JAPAN LINE 1/4000 MS INPUT  
INPUT\_VOLTAGE\_TIME\_CONSTANTS: ALPHA1=-0.17000E+03 ALPHA2=-0.32700E+07

\*\*\*TIME CONSTANT IN DECAY = 0.17000E+03\*\*\*\*

INPUT TIME STEP FROM 0 TO 5 MS = 0.5000E-07

TIME-VOLTAGE AREA OF INPUT = -0.96361E-05

(ALPHA1+ALPHA2)/ALPHA1= -0.10001E+01  
 -0.0 -0.150RF+00 -0.279RF+00 -0.3477E+00 -0.4801F+00 -0.5584F+00 -0.6251F+00 -0.6816F+00 -0.7296F+00 -0.7704F+00  
 -0.8050E+00 -0.8340F+00 -0.8594F+00 -0.8806E+00 -0.8986E+00 -0.9134E+00 -0.9269E+00 -0.9379E+00 -0.9472E+00 -0.9552E+00  
 -0.9619E+00 -0.9676F+00 -0.9725F+00 -0.9766E+00 -0.9801F+00 -0.9831E+00 -0.9856E+00 -0.9878E+00 -0.9896E+00 -0.9911E+00  
 -0.9924E+00 -0.9935E+00 -0.9945E+00 -0.9953E+00 -0.9960E+00 -0.9965E+00 -0.9970E+00 -0.9974E+00 -0.9978E+00 -0.9981E+00  
 -0.9983E+00 -0.9985E+00 -0.9987E+00 -0.9989E+00 -0.9990E+00 -0.9991E+00 -0.9992E+00 -0.9992E+00 -0.9993E+00 -0.9994E+00  
 -0.9994E+00 -0.9994E+00 -0.9995E+00 -0.9995E+00 -0.9995E+00 -0.9995E+00 -0.9995E+00 -0.9995E+00 -0.9995E+00 -0.9995E+00  
 -0.9995E+00 -0.9995E+00 -0.9995E+00 -0.9995E+00 -0.9995E+00 -0.9995E+00 -0.9995E+00 -0.9995E+00 -0.9995E+00 -0.9995E+00  
 -0.9995E+00 -0.9995E+00 -0.9995E+00 -0.9995E+00 -0.9995E+00 -0.9995E+00 -0.9995E+00 -0.9995E+00 -0.9995E+00 -0.9995E+00  
 -0.9994E+00  
 -0.9993E+00  
 -0.9993E+00 -0.9992E+00 -0.9992E+00 -0.9992E+00 -0.9992E+00 -0.9992E+00 -0.9992E+00 -0.9992E+00 -0.9992E+00 -0.9992E+00  
 -0.9992E+00 -0.9992E+00 -0.9992E+00 -0.9991E+00 -0.9991E+00 -0.9991E+00 -0.9991E+00 -0.9991E+00 -0.9991E+00 -0.9991E+00  
 -0.9991E+00 -0.9991E+00 -0.9991E+00 -0.9991E+00 -0.9991E+00 -0.9991E+00 -0.9991E+00 -0.9991E+00 -0.9991E+00 -0.9991E+00  
 -0.9990E+00  
 -0.9989E+00 -0.9989F+00 -0.9989F+00 -0.9989E+00 -0.9989E+00 -0.9989E+00 -0.9989E+00 -0.9989E+00 -0.9989E+00 -0.9989E+00  
 -0.9988E+00 -0.9988F+00 -0.9988F+00 -0.9988E+00 -0.9988E+00 -0.9988E+00 -0.9988E+00 -0.9988E+00 -0.9988E+00 -0.9988E+00  
 -0.9987E+00 -0.9987F+00 -0.9987F+00 -0.9987E+00 -0.9987E+00 -0.9987E+00 -0.9987E+00 -0.9987E+00 -0.9987E+00 -0.9987E+00  
 -0.9987E+00 -0.9987F+00 -0.9986E+00 -0.9986E+00 -0.9986E+00 -0.9986E+00 -0.9986E+00 -0.9986E+00 -0.9986E+00 -0.9986E+00  
 -0.9986E+00 -0.9986F+00 -0.9986F+00 -0.9985E+00 -0.9985E+00 -0.9985E+00 -0.9985E+00 -0.9985E+00 -0.9985E+00 -0.9985E+00  
 -0.9985E+00 -0.9985F+00 -0.9985F+00 -0.9985E+00 -0.9985E+00 -0.9985E+00 -0.9985E+00 -0.9985E+00 -0.9985E+00 -0.9985E+00

TIME OF INPUT VOLTAGE  
 0.0 0.500E-07 0.100E-06 0.150E-06 0.200E-06 0.250E-06 0.300E-06 0.350E-06 0.400E-06 0.450E-06

## BIBLIOGRAPHY

1. T. Ametani, "Single Propagation on a 500kV Untransposed Line: Field Test Results", CIGRE WG 13-05 13-74 (W.G. 05) 36 IWD, Oct. 1974.
2. T. Ametani et al, "Surge Propagation on Japanese 500 kV Untransposed Transmission Line", Proc. IEE, Vol. 121, pp. 136-138, 1974.
3. A. Greenwood, "Electrical Transients in Power Systems" Wiley Interscience, 1971.
4. H.W. Dommel, "Line constants of Overhead Lines: User's Manual", Method Analysis Group - BPA U.S. Department of Interior, June 1974.
5. H.W. Dommel, private communication, 1976.
6. J.R. Carson, "Wave Propagation in Overhead Wires with Ground Return", Bell System Technical Journal, Vol. 5, pp. 539-554, 1926.
7. S. Butterworth, "Electrical Characteristics of Overhead Lines", Electrical Research Association, Techn. Ref. O/T4, 1954.
8. D.E. Hedman, "Propagation on Overhead Transmission Lines II-Earth Conduction Effects and Practical Results", IEEE Trans. PAS, Vol. 84, pp. 205-211, March 1961.
9. W.C. Johnson, "Transmission Lines and Networks", McGraw-Hill, 1950.
10. A.E. Kennedy et al, "Experimental Research on Skin Effect in Conductor" AIEE Trans., pt. II, Vol. 34, pp. 1953-2018, 1915.
11. "Handbook of Mathematical Functions", Edited by M. Abramowitz and I.A. Stegun, published by U.S. Dept. of Commerce, pp. 384-385, 1964.
12. R.H. Galloway et al, "Calculation of Electrical Parameters for Short and Long Polyphase Transmission Lines", Proc. IEE, Vol. 111, No. 12, pp. 2051-2059, 1964.
13. H.W. Dommel, J.H. Sawada, "Report on the Calculation of Induced Voltages and Currents on Pipeline Adjacent to A.C. Power Lines" B.C. Hydro and Authorities CEA Contract No. 75-02, Aug. 1976.
14. H.W. Dommel, E.E. 463 and E.E. 553 Class Notes, U.B.C., 1976-77.
15. M.H. Hesse, "Electromagnetic and Electrostatic Transmission Line Parameter by Digital Computer", IEEE Trans. PAS, Vol. 82, pp. 282-290, 1963.
16. K.K. Tse, Private Communication, 1976.
17. D.F. Hedman, "Propagation on Overhead Transmission Lines I - Theory of Modal Analysis", IEEE Trans., PAS, Vol. 84, pp. 200-205, March 1965.

18. A. Budner, "Introduction of Frequency - Dependent Line Parameters into an Electromagnetic Transient Programme", IEEE Trans. PAS, Vol. 89, pp. 88-97, Jan. 1970.
19. W.G. Campbell, "Linear Algebra with Applications", Appleton Century Crofts, 1971.
20. U.B.C. Computing Centre Programme Library. "UBC MATRIX", Sept, 1976.
21. R.P. Gregory, "A Collection of Matrices for Testing Computational Algorithm", Wiley - Interscience, 1969.
22. F. Ayres, "Theory and Problems of Differential Equations", McGraw-Hill (Schaum Series) 1952.
23. E.W. Kimbark, "Electrical Transmission of Power and Signal", Wiley, 1958.
24. W.D. Stevenson, "Elements of Power System Analysis", McGraw-Hill, 1975.
25. R.K. Moore, "Travelling Wave Engineering", McGraw-Hill, 1960.
26. E. Groschupf "Simulation Transienter Vorgänge auf Leitungssystemen der Hochspannungs - Gleichstrom - und- Drehstrom - Übertragung", Ph.D. Thesis, Technischen Hochschule Darmstadt, 1975.
27. H.W. Dommel, "User's Instruction for Fourier Transformation Programme", Sept. 1976.
28. L. Lathi, "Signals, Systems and Communication", John Wiley & Sons, 1968.
29. W.S. Meyer, H.W. Dommel, "Numerical Modelling of Frequency-Dependent Transmission Line Parameters in an Electromagnetic Transient Programme", IEEE Trans. PAS, Vol. 74, pp. 1401-1409, 1974.
30. G.W. Swift, E.E. 571 Class Notes, 1977.
31. G.E.C. Measurements, "Protective Relays Application Guide", Tinlings Limited, 1976.
32. P.T.B. Adams et al. "Lightning Surges Propagation in 550 kV SF<sub>6</sub> Switchgear and Bus at B.C. Hydro Mica Generating Station", presented at the CEA Spring Meeting, Montreal, Quebec, March, 1977.